Interaction-dominant dynamics in human cognition: Beyond $1/f^{\alpha}$ fluctuation

Espen A. F. Ihlen and Beatrix Vereijken

Human Movement Science Programme, Norwegian University of Science and Technology, Trondheim, Norway

Address for correspondence:

Espen A. F. Ihlen

Human Movement Science Programme

Norwegian University of Science and Technology

Dragvoll Idrettssenter

N-7491 Trondheim

Norway

E-mail: espen.ihlen@ntnu.no

Tel: +47 735 98305

Fax: +47 735 91770

Keywords: response time, cognitive performance, multifractal, multiplicative interactions, interaction-dominant dynamics, $1/f$ fluctuation

Running title: Beyond $1/f^{\alpha}$ fluctuation

Abstract

It has been suggested that human behavior in general and cognitive performance in particular emerge from coordination between multiple temporal scales. In this paper, we provide quantitative support for such a theory of interaction-dominant dynamics in human cognition by using wavelet-based multifractal analysis and accompanying multiplicative cascading process on the response series of 4 different cognitive tasks, simple response, word naming, choice decision and interval estimation. Results indicated that the major portion of these response series had multiplicative interactions between temporal scales, visible as intermittent periods of large and irregular fluctuations (i.e., a multifractal structure). Comparing two component-dominant models of $1/f^{\alpha}$ fluctuations in cognitive performance with the multiplicative cascading process indicated that the multifractal structure could not be replicated by these component-dominant models. Furthermore, a similar multifractal structure was shown to be present in a model of self-organized criticality in the human nervous system, similar to a spatial extension of the multiplicative cascading process. These results illustrate that a wavelet-based multifractal analysis and the multiplicative cascading process form an appropriate framework to characterize interaction-dominant dynamics in human cognition. This new framework goes beyond the identification of $1/f^{\alpha}$ power laws and non-Gaussian distributions in response series as used in previous studies. Taken together, the present paper provides quantitative support for a paradigm shift towards interaction-dominant dynamics in human cognition.

Introduction

The emergence of spatial structures and temporal functions is a common feature of complex systems and reflects their ability to adapt to changes in their environments. The human nervous system is such a complex system consisting of about 10^{11} neurons with 10^{15} synapses (Kandel, Schwartz, & Jessell, 2000), and shifts in their coordinated and interconnected activity reveal changes in human cognition and behavior. The complexity seen in both the human nervous system and cognitive functions derives from the existence of numerous sub-structures and sub-functions that are distributed over multiple spatiotemporal scales. For example, the human cognitive function involves a microscopic scale of single neurons generating action potentials, but also a macroscopic scale of global activity in multiple neural structures generating behavior. Attempts are often made in both psychology and neuroscience to reveal the basic structural or functional architecture that can decompose the human nervous system and cognitive function into less complex pieces or components. In these so-called component-dominant views, focus lies on relationships between the simpler components within a single scale, for example the scale of molecules, neurons, or neural structures, while assuming that these are independent from relationships at other scales. However, when multiple scales of the phenomenon are interacting, this fundamental assumption of component-dominant views breaks down.

In contrast, so-called interaction-dominant views argue that the widely distributed ensembles of neural activity during task performance suggest inevitable interactions between the multiple spatial scales of the human nervous system. Furthermore, functional neural groups and pathways are thought to emerge through interactions between spatiotemporal scales that represent new behaviors or alternative ways to interact with a changing environment (Edelman, 1987). For example, the biochemical processes within a single neuron

can be seen as interactions between molecules that in turn define its firing pattern in interaction with its environment of adjacent neurons. The coordination or interaction of firing patterns within neural clusters defines the functions within and between neural structures that ultimately define human cognition and behavior in the context of an environment. Reversely, the environment constrains human behavior and the activity of the human nervous system through external stimulation. These external stimuli dissipate from macroscopic scales of the environment to microscopic scales of molecules, constraining the activity on each scale in between. Thus, the range from molecular interactions within single neurons to the interactions between the human nervous system and its environment, creates a continuum of interactions between the microscopic and macroscopic scales that are all part and parcel of human cognition. Consequently, according to interaction-dominant dynamics, theories of the human nervous system and cognition should not be decomposed into functions of encapsulated molecules, neurons, neural structures or behavior without considering their context or mutual interactions.

The existence of multiple scales reappears in the temporal domain of cognitive performance. Response series of a large number of trials can be decomposed into fast fluctuations and slow evolving trends under the assumption of the existence of independent cognitive time scales. For example, on short time scales of a few trials, the response series fluctuates in an irregular or noisy way thought to arise from the automatic and unconscious mechanisms of motor error correction (e.g., Gilden, 2001; Wing & Kristofferson, 1973). On longer time scales of hundreds or even thousands of trials, the same response series show additional slow regular trends thought to arise from the internal rhythm of the cognitive system (Gilden, 2001; Gilden, Thornton & Mallon, 1995) or from different levels of consciousness (Ward, 2002). The labeling of scale-dependent functions as levels of consciousness or metal sets, however, is only meaningful when they are mutually independent

and, as a result, a unique decomposition of the response series can be made. Only in this case can the measured response series be seen as a simple sum of scale-dependent sub-functions. In contrast to this component-dominant view, the presence of interactions between multiple time scales makes the scale-dependent sub-functions interdependent. This interdependency causes the breakdown of the fundamental assumptions of conventional statistical analyses and blends the abstract categories of level of consciousness, priming effects, motor error corrections and mental sets into one coherent concept of cognition. The main aim of the present paper is to introduce a new quantitative framework that can analyze human behavior as a coherent whole, thereby providing quantitative evidence for interaction-dominant dynamics in human cognition.

In the research on prolonged response series, two features are suggested to be omnipresent and therefore to represent the quantitative framework for the analysis of response tasks. First, when a response time series is decomposed by a Fourier transformation into a superposition of oscillations with frequency f, their squared amplitudes are shown to relate by a $1/f^{\alpha}$ power law (e.g., Farrell, Wagenmakers & Ratcliff, 2006; Kello, Anderson, Holden, & Van Orden, 2008; Kello, Beltz, Holden, & Van Orden, 2007; Thornton & Gilden, 2005; Torre & Delignières, 2008; Torre, Delignières, & Lemoine, 2007b; Torre & Wagenmakers, 2009; Van Orden & Holden, 2002; Van Orden, Holden, & Turvey, 2003, 2005; Wagenmakers, Farrell, & Ratcliff, 2004, 2005; Wijnants, Bosman, Hasselman, Cox, & Van Orden, 2009) The α exponent is shown to lie within the interval $0 < \alpha < 1$ in a broad range of cognitive tasks, including interval estimation, reaction time, mental rotation, lexical decision, serial search, and parallel search (e.g., Gilden, 1997, 2001). This implies that response series possess a long-range autocorrelation that defines the memory of the underlying cognitive system that can span thousands of trials. Thus, the presence of $1/f^{\alpha}$ fluctuation is illustrated by a regular, less-than-random structure of the response series and implies that it cannot be considered as

random noise around an average response time. Gilden and coworkers (Gilden, 2001; Gilden et al., 1995; Thornton & Gilden, 2005) suggested that cognitive performance results from $1/f^{\alpha}$ fluctuation in the internal clock of the cognitive system combined with white noise in the motor execution system or as priming effects. A similar approach has been taken in the investigation of timing tasks such as finger tapping, where a motor error correction term is defined as differentiated white noise (Wing & Kristofferson, 1973) and added to models of $1/f^{\alpha}$ fluctuation (e.g., Delignières, Torre, & Lemoine, 2008; Torre & Delignières, 2008; Torre & Wagenmakers, 2009). Ward (2002) has suggested that $1/f^{\alpha}$ fluctuation originates from the sum of autoregressive processes, where each scale-dependent process is describing conscious, unconscious, and preconscious components of the cognitive system. These components are also hypothesized to be the output of independent groups of neurons in the central nervous system (Chen, Ding, & Kelso, 2001; Ding, Chen, & Kelso, 2002; Ward, 2002).

In contrast to the above component-dominant perspectives, Van Orden et al. (2003, 2005), followed by Kello et al. (2007), proposed a paradigm shift from considering $1/f^{\alpha}$ fluctuation as a quantitative by-product of scale-dependent processes to seeing the α exponent as a universal signature of interaction-dominant dynamics (Jensen, 1998). These authors suggested that human cognition and behavior self-assemble critical states, allowing for flexible adaptation to changing circumstances. This interaction-dominant theory was inspired by the contemporary inter-disciplinary literature of self-organizing critical systems that produce $1/f^{\alpha}$ fluctuation as a statistical output (Bak, 1996; Jensen, 1998). In a reaction to this proposal, Wagenmakers and colleagues (Torre & Wagenmakers, 2009; Wagenmakers et al., 2004, 2005) argued that this view – though exciting – is premature, as $1/f^{\alpha}$ fluctuation can also be generated by the far simpler component-based models mentioned above. Consequently, a $1/f^{\alpha}$ power law in itself cannot distinguish between component- and interaction-dominant dynamics. For instance, spectral portraits always involve a Fourier

transformation which assumes independence between the oscillations (i.e., non-interacting components). Yet, it is noteworthy that independence between oscillations has not been demonstrated empirically. Thus, $1/f^{\alpha}$ power laws, thought to be ubiquitous in human performance (e.g., Kello et al., 2007; Van Orden et al., 2003, 2005), are neither necessary nor sufficient evidence of interaction-dominant dynamics.

The second feature of prolonged response series is that they possess a non-Gaussian distribution with heavy tails (Holden, 2002; Holden, Van Orden, & Turvey, 2009). These heavy tails arise from extreme response intervals and are often eliminated as singular or rare events. But even when response times more than three standard deviations from the average are eliminated, heavy tails remain present in the probability density function. The component-dominant models of human cognition cited above fail to reproduce the non-Gaussian distribution seen in the response series since they are based on a superposition of scale-dependent sub-processes that are Gaussian distributed. In contrast, non-Gaussian probability density functions like log-normals or power laws are shown in the interdisciplinary literature to arise from multiplicative noise where the sub-processes are interdependent (e.g., Sornette, 2004). However, it is problematic to unequivocally equate the shape and width of a particular non-Gaussian probability density function with interaction or coordination between multiple temporal scales of a response series. The main problem of equating multiplicative interactions with non-Gaussian distribution is that the probability density function does not contain information about the temporal ordering of the extreme trials within its tails. This means that even though multiplicative interactions imply a non-Gaussian probability density function, the reverse statement is not necessarily true.

The fundamental insufficiency of unequivocally equating the presence of a $1/f^{\alpha}$ power law and a non-Gaussian probability density function with the presence of multiplicative interactions across temporal scales can be eliminated by a third, more general feature of

complex systems, namely intermittency. In a response series, intermittency is visible as distinct periods of large and irregular performance variability that reflects the waxing and waning of the subjects' attention to the stimuli or their intention to act according to the experimental instructions. These intermittent fluctuations in a response series imply an inhomogeneous distribution of response time variability. The inhomogeneous distributed variability within the response series leads to a time-dependency in both the probability density function and α exponent (i.e., local regularity). However, the conventional analyses and models of both $1/f^{\alpha}$ power law and non-Gaussian probability density function of a response series assume that the α exponent is homogenous in time, and they are therefore blind to the presence of intermittency (Mandelbrot, 1997). Intermittent behavior of complex systems has therefore been viewed as a property that is difficult to quantify by a single statistical parameter.

The solution to this fundamental problem was developed by Mandelbrot (1974) through stationary models of multiplicative interactions between scale-dependent vertexes in fluid turbulence. These models were termed multiplicative cascading processes and classify intermittency in phenomena as diverse as stock market fluctuation (Mandelbrot, 1997), heart rate variability (Ivanov, Rosenblum, Peng, Mietus, Havlin, Stanley, & Goldberger, 1996; Ivanov, Amaral, Goldberger, Havlin, Rosenblum, Struzik, & Stanley, 1999; Lin, 2003), stride rate variability (Scafetta, Griffin, & West, 2003), earthquakes (Sornette & Ouillon, 2005), galaxy distributions (Fang, 2006), wind speed fluctuation (Kavasseri & Nagarajan, 2005), impact fragmentations (Katsuragi, Sugino, & Honjo, 2003), and other complex phenomena in physics and chemistry (cf. Stanley & Meakin, 1988). Common for these models is that the intermittent structure in time or space is defined by multiplicative interactions that transport energy and information across multiple spatiotemporal scales. Furthermore, the intermittent structure generated by multiplicative interactions is the generic concept of multifractality and

strongly suggests emergent changes in cognitive performance. In the current paper, we will illustrate that the generation of intermittent fluctuation by multiplicative interactions between the temporal scales of cognitive performance can be investigated quantitatively through multifractal analyses.

The aim of this paper is to outline a sufficient and more complete quantitative framework of interaction-dominant dynamics in human performance by equating interaction-dominant dynamics with interaction, coordination, and interdependence between multiple scales in both time and space. As this is relatively new in psychological literature, the method section presents an introduction of multifractal analysis and multiplicative cascading processes. Although the analyses are rather technical, they will become clearer in the results section where the quantitative framework is tested on two existing data sets in the literature. One data set is based on a simple response task, a choice decision task, and an interval estimation task (Wagenmakers et al., 2004), the other data set on a simple response task and a word naming response task (Van Orden et al., 2003).

Methods

The method section consists of several parts that together introduce a quantitative framework for investigating interaction-dominant dynamics in human performance. We quantitatively define the presence of multiplicative interactions between temporal scales, causing intermittency in response series, under the heading “The multifractal spectrum”. The computation of the multifractal spectrum is based on wavelet extensions of conventional Fourier transformation, which are introduced first under the heading “The wavelet lens”. The presence of multiplicative interactions in a response series is then modeled as a ‘Multiplicative cascading process’ under the heading with the same name, which is known to

produce the multifractal structure of a time series (Muzy & Bacry, 2002). A surrogate test is subsequently introduced under the heading "Validation of multiplicative interactions" to validate the presence of multiplicative interactions in the response series. A wavelet-based statistical test is finally introduced in the last part, "Statistical analysis of multiplicative interactions", to identify inhomogeneous wavelet variance, as the latter is a necessary consequence of multiplicative interactions. For the technically advanced reader, the mathematical relationship between the multifractal spectrum and the multiplicative cascading process are presented in the Appendix, together with the algorithms for the wavelet-based deduction of the multifractal spectrum.

The wavelet lens: Response series are typically decomposed into a sum of oscillations with wavelength $\Delta t = 1/f$ in order to define the presence of the conventional $1/f^{\alpha}$ power law. This decomposition is performed by a mathematical lens called a Fourier transformation. The fundamental assumption of the Fourier transformation is that the amplitude $A_{\Delta t}$ of each oscillation is independent of the others and thus without amplitude modulation in time (see Figure 1A). However, this fundamental assumption is violated by the presence of so-called laminar and intermittent periods in the response series, consisting of small, regular fluctuations and large, irregular fluctuations, respectively. In the intermittent periods, the amplitude of the oscillations suddenly increase for the short wavelengths Δt. This implies that the $1/f^{\alpha}$ power law becomes time dependent with the single α exponent deduced by the Fourier lens defining only the average structure or regularity of the intermittent response series. Intermittency, or local regularity of the response series, thus lies within the "*blind spots*" (Mandelbrot, 1997, p. 163) of the Fourier lens. However, these spectral blind spots can be revealed by a wavelet transformation, as illustrated by several successful applications in a

range of scientific disciplines over the last decade (e.g., Aldroubi & Unser, 1996; Hubbard, 1998; Prasad & Lyengar, 1997; Van den Berg, 1999; Walczak, 2000).

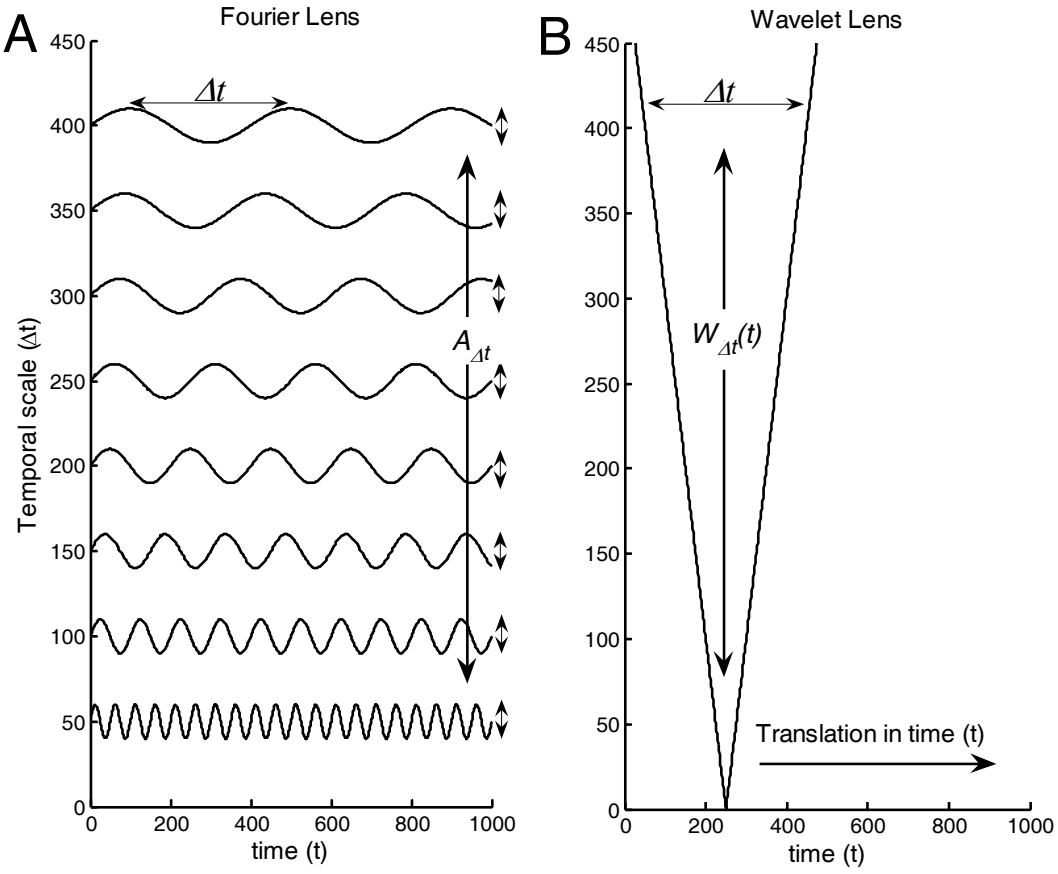

Figure 1. (A) The response series is decomposed into a series of sine waves by the conventional Fourier lens. Their stationary amplitude $A_{\Delta t}$ is a result from the independency between the sine waves with different wavelength Δt. (B) The wavelet lens decomposes the response series into wavelet coefficients $W_{\Delta t}(t)$ within a cone. The amplitude modulation of the sine waves caused by interactions between the temporal scales Δt is then captured by translating the cone in time. Thus, wavelet transformation can capture the interaction-induced temporal changes of the sine wave amplitudes which are not possible through the Fourier lens.

The wavelet transformation fits a waveform of width Δt to the response series in each time instant t. For each fit, the wavelet coefficients $W_{\Delta t}(t)$ define the amplitude of the waveform and decompose the response series into a time-scale plane (see Figure 1B). In intermittent periods of large response variability, the wavelet coefficients will be large across

scales Δt, while it becomes small in the laminar periods of small variability. Thus, the alignment of large wavelet coefficients into distinct cones in the time-scale plane points to intermittent periods of large performance variability (see Figure 1B and upper panel in Figure 2B). Consequently, wavelet transformations can identify interactions between the amplitudes of oscillations across scales Δt causing intermittent, emergent or coherent periods of large fluctuations within the response series.

In the present paper, two different wavelet algorithms will be used to cross-validate the presence of intermittency. The Continuous Wavelet Transformation (CWT) uses a Morlet waveform to decompose the response series into a continuous range of temporal scales (Goupillaud, Grossmann, & Morlet, 1984) (see upper panels in Figure 2). In addition, the Maximum Overlap Discrete Wavelet Transform (MODWT) with an 8th order least asymmetric waveform is used to decompose the response series into a discrete range of scales (Daubechies,1992; Mallat, 1989, 1999; Percival & Walden, 2000) (see lower panels in Figure 2). See the Appendix for the technical details of the wavelet algorithms.

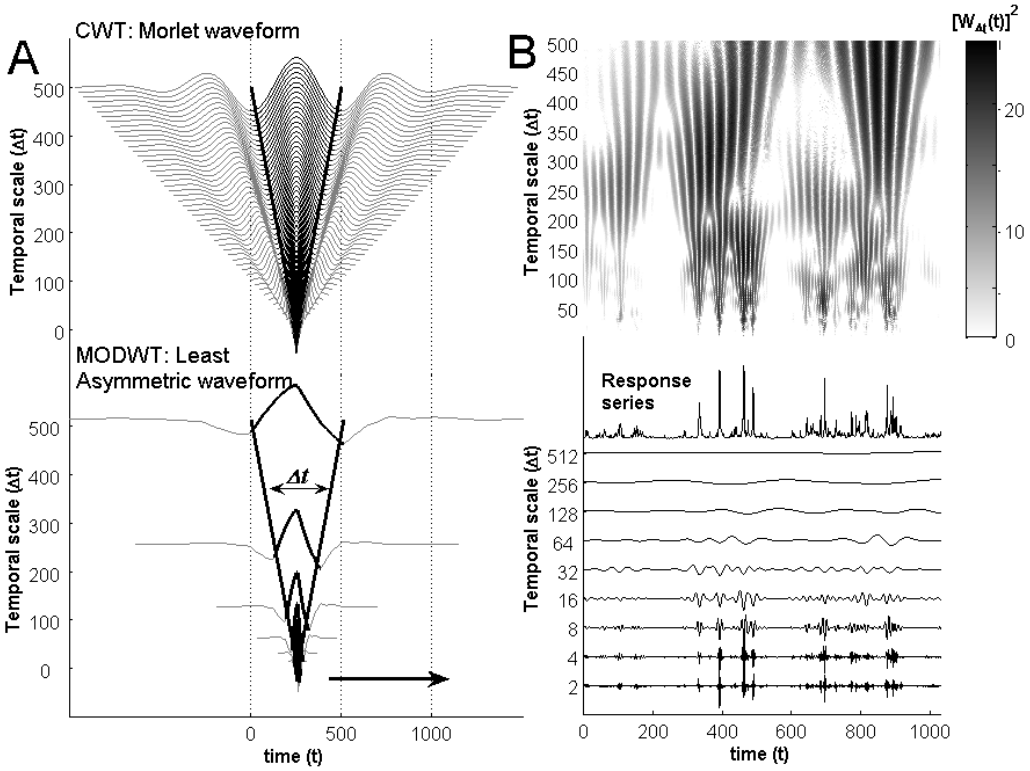

Figure 2. (A) The *upper panel* illustrates a Morlet waveform for the continuous wavelet transformation (CWT). The waveform is centered and scaled according to the width Δt of the wavelet cone (*black lines*). The *lower panel* illustrates a Least Asymmetric waveform for the maximum overlap discrete wavelet transformation (MODWT). In contrast to the CWT, the latter waveform is scaled for discrete scales $\Delta t = 2, 4, 8, \ldots, 512$. Note that within the wavelet cone, both the Morlet and Least Asymmetric waveform resemble the sine wave used in conventional Fourier transformation. (B) The upper panel illustrates the wavelet variance $[W_{\Delta t}(t)]^2$ in the time-scale plane obtained from the CWT. The *lower panel* defines the scale-dependent processes obtained by the inverse MODWT for the temporal scales $\Delta t = 2, 4, 8, \ldots, 512$.

The multifractal spectrum: The identification of conventional $1/f^{\alpha}$ fluctuation in the response series by a power spectrum analysis, detrended fluctuation analysis, rescaled range analysis, scaled window variance analysis or dispersion analysis, are all based on temporal scaling of the response time variance (e.g., Chen, Ding, & Kelso, 1997, 2001; Delignières, Lemoine, & Torre, 2004; Delingières et al., 2008; Gilden, 1997, 2001; Gilden et al., 1995; Kello et al., 2007; Lemoine, Torre, & Delignières, 2006; Pressing, 1999; Pressing & Jolley-Rogers, 1997; Torre, Delignières, & Lemoine, 2007a, 2007b; Van Orden & Holden, 2002; Van Orden et al., 2003, 2005; Wagenmakers et al., 2004, 2005). These analyses thus assume that the response series has a stationary Gaussian probability density function such that it possesses homogenously distributed fluctuations. However, when the participants' attention to stimuli or commitment to the response task changes, the fluctuations will be inhomogeneously distributed, visible as intermittent periods of large performance variability. In this case, the response series will possess a probability density function with non-Gaussian heavy tails (e.g., Holden et al., 2009). Consequently, it is no longer sufficient to analyze the scaling of the variance (i.e., second order statistical moment) and the entire probability density function defined by all q-order statistical moments should be considered. The conventional $1/f^{\alpha}$ power

law[1] can then be generalized for an arbitrary non-Gaussian probability density function by the q-order moments of wavelet coefficients $W_{\Delta t}(t)$ (e.g., Abry, Flandrin, Taqqu, & Veitch, 2000, 2002; Muzy, Bacry, & Arneodo, 1991, 1993, 1994):

$$\frac{1}{N}\sum_{t=1}^{N}\left|W_{\Delta t}(t)\right|^{q} \propto \Delta t^{\zeta(q)} \tag{1}$$

where N is the number of trials within the response series. The spectrum of exponents $\zeta(q)$ defines, for small q, the regularity of the laminar periods of little performance variability and, for large q, the regularity of intermittent periods of large performance variability. In the special case when $q = 2$, the multiscaling exponent $\zeta(q)$ coincides with the α exponent and defines the average structure or regularity of the response series. Furthermore, when multifractality is present the spectrum of exponents $\zeta(q)$ is nonlinearly convex, which implies that the intermittent periods of large performance variability will possess a more irregular structure (i.e., a zigzag pattern) compared to laminar periods of little variability. Thus, in a cognitive task multifractality will be present because large increases in response times have to be counter-acted by large decreases in order not to breach the time limit of the task. This generates a less correlated zigzag pattern in the intermittent periods of large response time variability, defined by a decrease in a local h exponent. In contrast, during laminar periods of little response time variability the structure of the response series will evolve freely with little influence of the time limits of the experiment. In this case, the structure will be correlated and defined by an increase in the local h exponent. Consequently, the distribution of h exponents summarizes the temporal change in regularity or patchiness in the response series, which arises from the coordination between its temporal scales. This distribution is called a

[1] The inverse frequency $1/f$ is equal to the temporal scale Δt.

multifractal spectrum $D(h)$, which is related to $\zeta(q)$ by the following Legendre transformation (e.g., Riedi, 2002):

$$h = \frac{d\zeta(q)}{dq}$$
$$D(h) = qh - \zeta(q) \tag{2}$$

The width $h_{max} - h_{min}$ of the multifractal spectrum $D(h)$ defines the amplitude difference between the variability in the intermittent and in the laminar periods within the response series. As a result, the multifractal spectrum width $h_{max} - h_{min}$ quantifies the influence of the multiplicative interaction, or coordination, between the multiple time scales of the response series. When the multifractal spectrum $D(h)$ collapses into a single h (i.e., $h_{max} - h_{min} = 0$), the response series is monofractal and no coordination between the temporal scales is present. In this particular case, there will be no emergence of cognitive functions seen as intermittent change in the performance variability and the response series will thus possess a homogeneous fluctuation.

To summarize, intermittency is the quantitative concept of emergent change in behavior defined through the inhomogeneously distributed variability within the response series. These changes might be fundamental shifts in the cognitive system in order to adapt to changes in its complex environment. These same intermittent changes can be quantitatively identified as the coordination of the amplitudes of the wavelet coefficients across multiple time scales, as illustrated in Figure 2B and summarized statistically in the multifractal spectrum $D(h)$. The multifractal spectrum width $h_{max} - h_{min}$ therefore quantifies the amount of emergent changes in the participant's commitment, attention to stimuli, or intention to act within the constraints of the cognitive task.

Multiplicative cascading process: In order to model an intermittent response series, a fundamental principle for the interactions across multiple time scales is necessary. Such a fundamental principle can be defined as a *multiplicative cascading process* for which the general statistical framework was introduced by Mandelbrot (1997) in econometrics and further developed by Muzy and Bacry (2002) and Chainais, Riedi, and Abry (2005). The multiplicative cascading process is defined by the product of the multipliers within the wavelet cone in the time-scale plane illustrated in Figure 1B. When the products of multipliers becomes small in the scale limit $\Delta t \rightarrow 0$ (i.e., the tip of the translating cone in Figure 1B), it reflects laminar periods of little performance variability. In contrast, intermittent periods of large performance variability emerge when the same product of multipliers becomes large. The crucial property of the multiplicative cascading process is that the interaction multipliers have a stationary (i.e., time-independent) distribution in the time-scale plane even though both its local regularity (i.e., h exponent) and its probability density function are non-stationary (i.e., time-dependent). Consequently, the probability density function of the interaction multipliers quantifies the fundamental principle of coordination of the multiple temporal scales within the multiplicative cascading process. This means that even though the sub-processes or components within the response series change in time because of their mutual coordination, the nature of the coordination itself is independent of time. The mathematical definition of the multiplicative cascading process is given by equations (A2) - (A7) together with Figures A1-3 in the Appendix.

The distribution of interaction multipliers in the multiplicative cascading process is mathematically directly related to the multifractal spectrum. The alignment of small and large multipliers in the laminar and intermittent periods is equivalent to the alignment of small and large wavelet coefficients such that the distribution of the interaction multipliers in the time-scale plane is equivalent with the multifractal spectrum. Consequently, the multifractal

spectrum quantifies the nature of the coordination between the multiple time scales of a response series, which is not possible through a single α exponent. Figure 3A illustrates this point further by a MODWT decomposition of two time series with equal α exponent ($\alpha = 1$), where the upper panel is a multiplicative cascading process with multifractal spectrum width $h_{max} - h_{min} = 1.2$, while the lower panel represents a monofractal series or pink noise with $h_{max} - h_{min} = 0$. The difference between laminar and intermittent periods in the former is most distinct at the smallest scales (i.e., $\Delta t = 2$, 4 and 8) where the corresponding probability density function possesses non-Gaussian heavy tails (see upper panel in Figure 3B). The magnitude of these heavy tails defines the width of the distribution of interaction multipliers in the time-scale plane and thus the width $h_{max} - h_{min}$ of the multifractal spectrum $D(h)$ (see Figure 3C). In contrast, the MODWT decomposition of pink noise (see lower panel of Figure 3A) has no intermittent periods, such that the wavelet coefficients are Gaussian distributed (see lower panel of Figure 3B) and the multifractal spectrum collapses into a single point (see the gray dots in the upper left part of Figure 3C). As a result, the multifractality represents the multiplicative interactions between temporal scales seen in the alignment of the large wavelet coefficients (see upper panel of Figure 3A), while the absence of multiplicative interactions in a monofractal time series implies the lack of coordination between its temporal scales with no alignment of the coefficients (see lower panel of Figure 3A). In sum, Figure 3 illustrates that the coordination of multiple time scales revealed by the wavelet transformation lies within the blind spot of the Fourier lens.

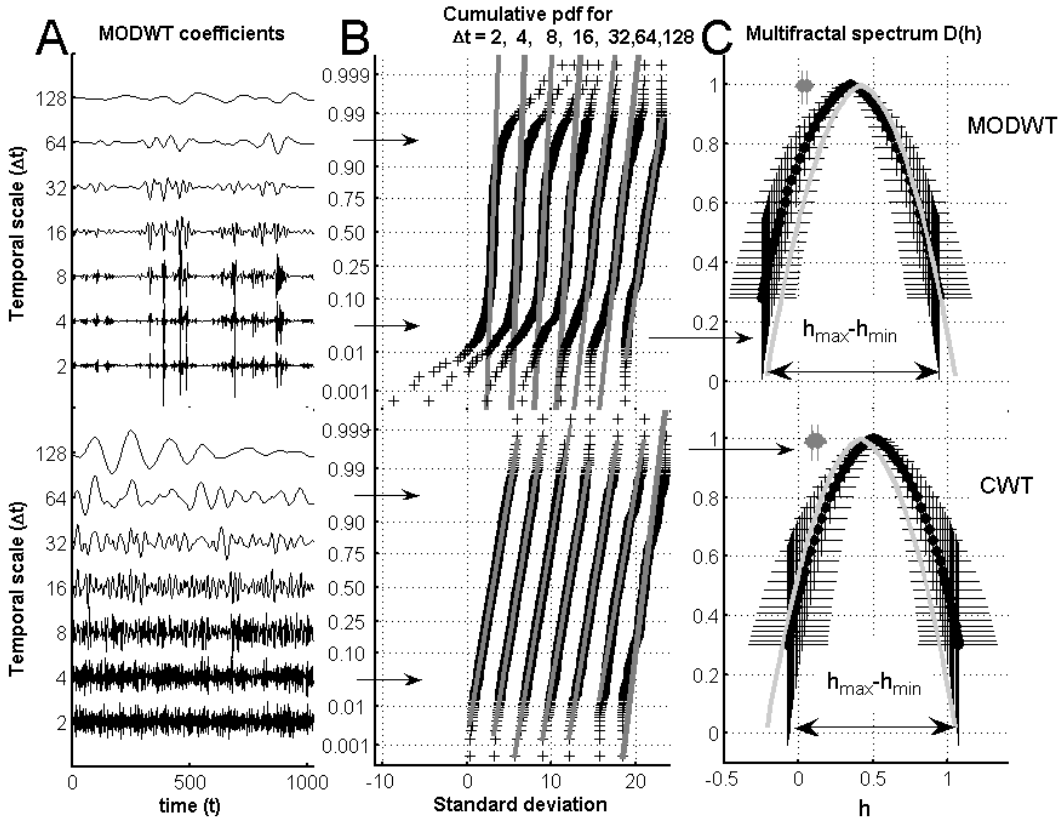

Figure 3. (A) The MODWT coefficients for the multiplicative cascading process (*upper panel*) and monofractal fluctuations or pink noise (*lower panel*) for scales Δt = 2, 4, 8, 16, 32, 64, and 128. The *upper panel* shows time-dependent changes in the coefficients that originate from the cumulative product of interaction multipliers, especially for the small scales $\Delta t \rightarrow 0$. (B) The cumulative probability density function (pdf) of the MODWT coefficients, displayed in log-coordinates in order to visualize the tails. For the multiplicative cascading process (*upper panel*), a non-Gaussian distribution of the MODWT coefficients is present when $\Delta t \rightarrow 0$ (i.e., deviations from the *gray lines*). For the pink noise (*lower panel*), the distribution is approximately Gaussian (*gray lines*) for all scales Δt. (C) The multifractal spectrum $D(h)$ estimated by the wavelet coefficients of MODWT (*upper panel*) and CWT (*lower panel*) through equations (1) and (2). The *vertical* and *horizontal black bars* are ±1 standard deviation for the $D(h)$ and h, respectively, of 100 realizations of the multiplicative cascading process. The *gray arc* defines the analytical result of this model and is within 1 standard deviation of the estimations. The small cluster of gray bars to the left of the arc in both panels defines the monofractal fluctuations or pink noise where the spectrum has collapsed into a single point $D(h) = 1$.

Validation of multiplicative interactions: In the above section, interaction-dominant dynamics was equated with multiplicative interactions between temporal scales of the response series and quantified by the width of the multifractal spectrum. It is important to validate that the obtained multifractal spectrum width $h_{\max} - h_{\min}$ originates from the interactions between the multiple time scales and not from the mere presence of $1/f^{\alpha}$ power law and a non-Gaussian probability density function. This validation is possible by generating an ensemble of surrogate series in which the non-Gaussian distribution and $1/f^{\alpha}$ fluctuation are preserved while the interactions between the multiple scales are eliminated. When there is a significant difference between the multifractal spectrum width $h_{\max} - h_{\min}$ of the response series and the average spectrum width of the ensemble of surrogates, then interactions between multiple time scales are present.

For each response series, an ensemble of 30 surrogates was generated. Each surrogate was generated through an Iterated Amplitude Adjusted Fourier transformation developed by Schreiber and Schmitz (1996). First, the rank ordering is stored of the amplitudes of both the response series and its power density spectrum obtained through a fast Fourier transformation. Secondly, the response series are randomly shuffled. Thirdly, an iterative procedure is initiated where the spectral amplitudes of the fast Fourier transformation of shuffled series are substituted with the stored spectral amplitudes of the original response series. The inverse fast Fourier transformation is then applied and the surrogate series are obtained in which the amplitudes are ranked as in the original response series. In the present study, the third step is iterated 500 times for all surrogate series to make sure that they obtain both a Fourier spectrum and a probability density function that are equal to the original response series. Multiplicative interactions between the temporal scales of the response series are present when the multifractal spectrum width of each response series is outside the 95 % confidence interval of the surrogate ensembles' width ($p < 0.05$).

The important feature of the above procedure is that possible correlations between the Fourier phases are eliminated in step three. This means that the procedure eliminates the alignment of large wavelet coefficients seen in the upper panel of Figure 3A and therefore the intermittent structure of the response series. There are two cases in which there are no multiplicative interactions between temporal scales in the response series. The first case is when the multifractal spectrum width is within the ensemble of surrogate series but not equal to zero. In this case, the multifractality is induced by a stationary non-Gaussian probability density function of the response series rather than by interactions between multiple scales. Consequently, the response series can be characterized by the non-Gaussian function together with the $1/f^{\alpha}$ power law since the extreme trials are singular random events rather than intermittent periods of large variability. In the second case, the multifractal spectrum width is approximately zero and within the ensemble of surrogates. Only in this special case, the response series has a non-intermittent structure characterized by the $1/f^{\alpha}$ power law alone.

Statistical analysis of multiplicative interactions: The presence of multiplicative interactions between temporal scales of the response series implies that the heavy tails of wavelet coefficients in the upper panel of Figure 3B increase when $\Delta t \rightarrow 0$. If, on the other hand, the response series are sufficiently quantified by the $1/f^{\alpha}$ power law alone, the coefficients should be independent, Gaussian-distributed variables on all scales as in the lower panel of Figure 3B, implying that no interactions are present. This can be tested statistically by a cumulative sum of squares-based statistics (i.e., *D*-statistics) of the wavelet coefficients (Percival & Walden, 2000; Whitcher, 1998). The *D*-statistics compare the variance of wavelet coefficients (i.e., $[W_{\Delta t}(t)]^2$) of the response series at each temporal scale Δt, with 1000 series of Gaussian noise (see equations (A18)-(A22) in the Appendix). If a significantly large portion (i.e., > 950/1000, with $p < 0.05$) of these series has equal or lower wavelet variance, then the

response series contains non-Gaussian distributed wavelet coefficients significantly different from those of conventional $1/f^{\alpha}$ fluctuation. In that case, the inhomogeneous distribution of wavelet coefficients of the multiplicative cascading process in the upper panel of Figure 3A has more pronounced heavy tails at the smallest temporal scales when $\Delta t \rightarrow 0$. In contrast, the coefficients of monofractal pink noise in the lower panel of Figure 3A are distributed homogenously in time and are indifferent from Gaussian noise.

The same wavelet-based statistical test can also test the ability of cognitive performance models to replicate the presence of inhomogeneous distributions of wavelet coefficients in the time-scale plane of each response series. This is obtained by using the wavelet coefficients of 1000 realizations of the statistical model instead of Gaussian noise. If a significantly large portion (i.e., > 950/1000, with $p < 0.05$) of 1000 realizations of the model has equal or lower wavelet variance compared to each response series, then the model is not able to replicate the interactions across its temporal scales. In the present study, we will compare the superposition of $1/f^{\alpha}$ fluctuation and white noise (Gilden et al., 1995; Gilden, 2001; Thorton & Gilden, 2005), an aggregated autoregressive process (Wagenmakers et al., 2004; Ward, 2002), and the presently introduced multiplicative cascading process with respect to their ability to replicate the intermittent property of response series.

Results and discussion

The results section consists of three major parts, each concluded by a short discussion. In the first part, Interaction-dominant dynamics in cognitive performance, we will apply the multifractal analysis to the existing data sets of Wagenmakers et al. (2004) (*Data set 1*) and Van Orden et al. (2003) (*Data set 2*) in order to investigate the presence of multiplicative interactions between the temporal scales of a single response series. In the second part,

Component- versus interaction-dominant models of cognitive performance, we will compare the results of the multifractal analysis to the most common component-dominant models in the literature and to the presently suggested multiplicative cascading process. In the third part, Interaction-dominant dynamics in the nervous system, we will extend the quantitative framework of interaction-dominant dynamics to the self-assembled neural activity in the nervous system.

Interaction-dominant dynamics in cognitive performance

Data set 1: Wagenmakers et al.'s (2004) data set[2] consists of 6 subjects participating in 3 different cognitive tasks, a simple response, a choice decision, and an interval estimation task. Arabic numerals 1 to 9 were presented as visual stimuli on a computer screen until a response was registered. In the simple response task, the participants responded as fast as possible by pressing '/' with their right index fingers. In the choice decision task, the participants responded as fast as possible without error by pressing '/' with the right index finger when an even number was displayed and 'z' with the left index finger when an odd number was displayed. In the time interval estimation task, a one second time interval was estimated by the participants by pressing the '/' key with their right index finger to mark the duration of the interval after stimulus onset. Furthermore, each of the three tasks had two within-task conditions, with either a short (randomized 200-600 ms) or a long (randomized 800-1200 ms) 'response to stimulus interval' (RSI). The ordering of the short and long RSI was randomized for each participant and task. In all, Wagenmakers et al.'s (2004) data set contained 6x3x2 = 36 response series of 1024 trials differing only in task instruction and RSI. All participants conducted the 3 tasks x 2 RSI sessions within one week with no more than 1 session per day,

[2]To be found at http://users.fmg.uva.nl/ewagenmakers/fnoise/noisedat.html

where the ordering of the task was set by the employment of a counter-balanced, Latin-square design. Response times below 100 ms were considered to be caused by anticipation of the next stimulus and eliminated from the data set before further analysis (cf. Wagenmakers et al., 2004).

Multiplicative interactions in data set 1: Figure 4 illustrates representative examples of response series in the simple response (upper left panel) and in the interval estimation (upper right panel) task, with corresponding decomposition into the time-scale plane by the CWT (lower panels). The simple response task has more pronounced intermittent periods of large performance variability compared to the interval estimation task (see upper panels in Figure 4). This implies that the wavelet variance of the simple response task is less homogeneously distributed compared to the interval estimation task, which is observable as larger light areas especially at the finest scales, i.e., $\Delta t \rightarrow 0$ (see lower panels). This difference becomes clearer in the bottom panel of Figure 5A, which shows that the wavelet coefficients of the MODWT for the simple response task have a less homogeneous fluctuation at the finest scales (Δt = 2, 4, and 8 trials) compared to the interval estimation task. The inhomogeneous fluctuation in the simple response task leads to increases in the influence of heavy tails in the corresponding probability distribution as $\Delta t \rightarrow 0$ (see upper panel in Figure 5B). This again implies a significantly ($p < 0.05$) wider multifractal spectrum width $h_{max} - h_{min}$ than the mean ensemble width of the surrogates (see Figure 5C, upper panel). In contrast, the response series of the interval estimation task has more homogeneous fluctuation of the wavelet coefficients and therefore an approximately Gaussian distribution for all temporal scales Δt, which implies an approximately monofractal spectrum (i.e., $h_{max} - h_{min} \approx 0$). The multifractal spectrum was computed for both the continuous (CWT, black circles in Figure 5C) and the maximum overlap discrete wavelet transformation (MODWT, black squares in Figure 5C), and there

was a high correlation ($R = 0.82$, $p < 0.0001$) between the estimations of their widths $h_{\max} - h_{\min}$.

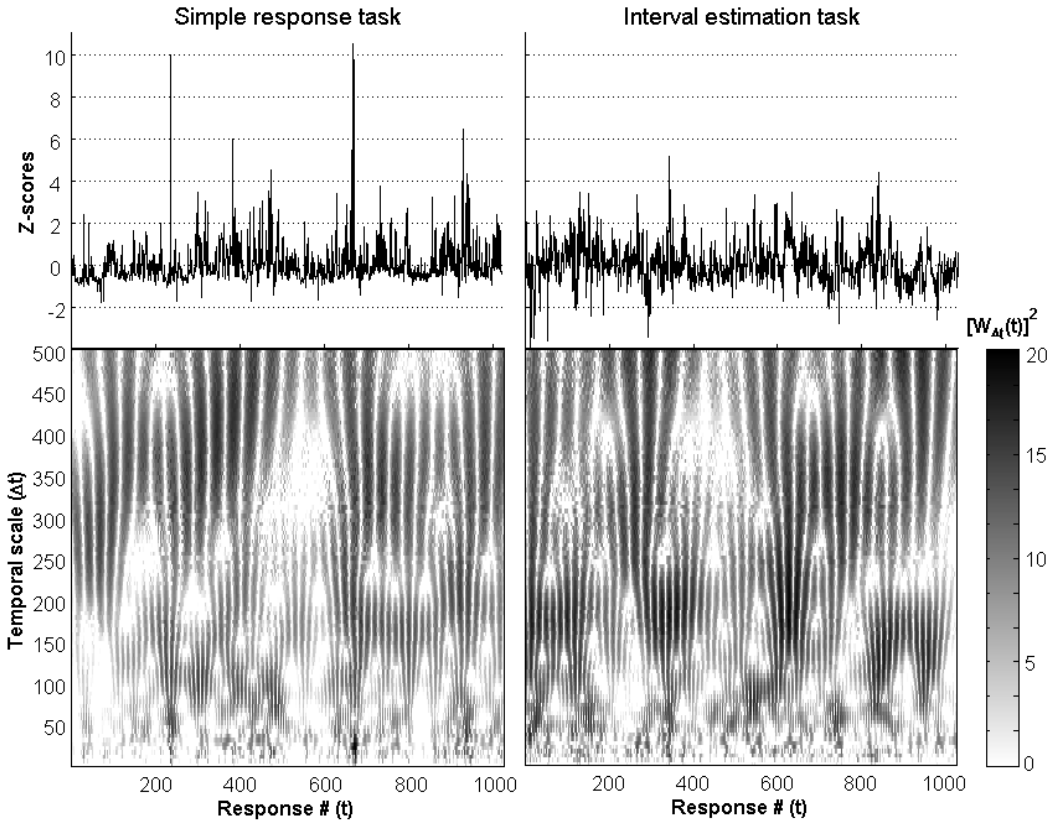

Figure 4. Representative examples of response series for the simple response task (*upper left panel*) and interval estimation task (*upper right panel*) in Z-scores. The bottom panels represent the power spectra $[W_{\Delta t}(t)]^2$ of the same response series when resolved into the time-scale plane.

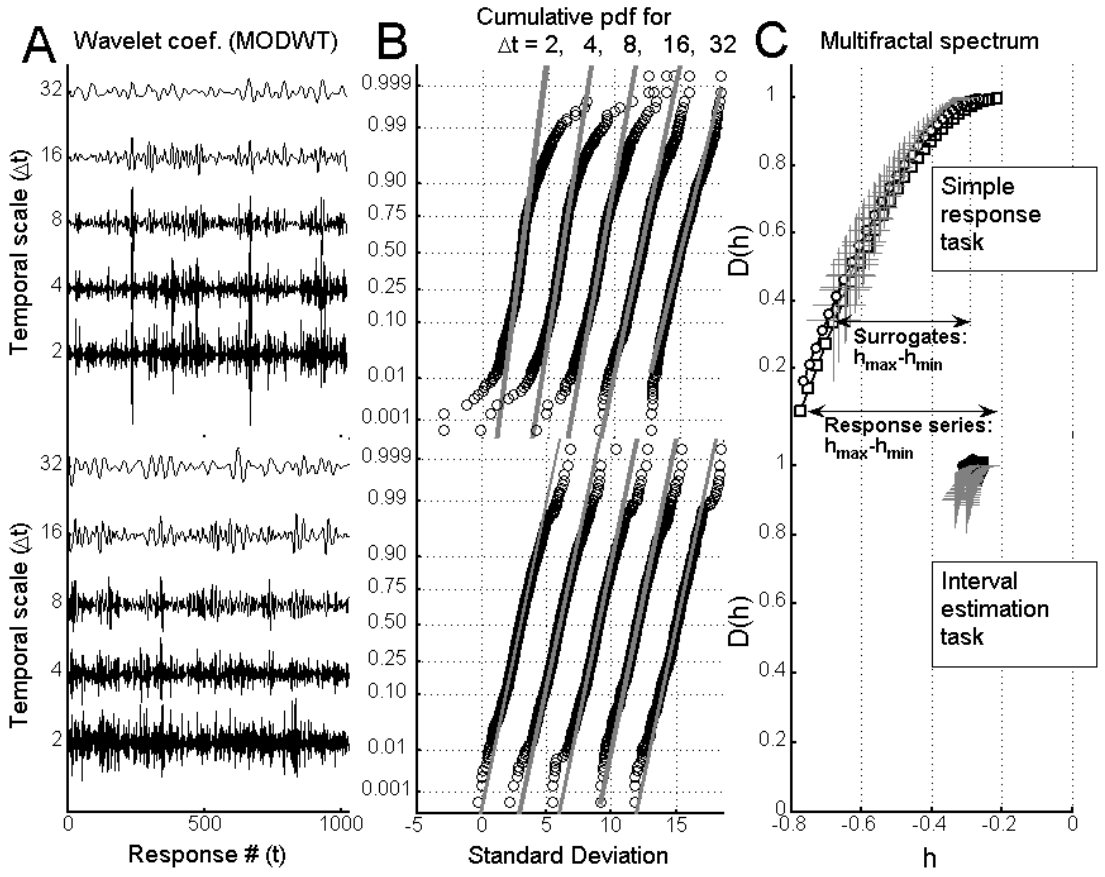

Figure 5: (A) A representative example of the MODWT coefficients for temporal scales Δt = 2, 4, 8, 16, and 32 trials for the simple response task (*upper panel*) and interval estimation task (*lower panel*) (as in Figure 4). The simple response task has a less homogeneous variance compared to the interval estimation task when $\Delta t \rightarrow 0$, arising from multiplicative interactions. (B) The cumulative probability density function (pdf) of the MODWT coefficients for the simple response task (*upper panel*) and interval estimation task (*lower panel*). The non-Gaussian heavy tails of the former increase when $\Delta t \rightarrow 0$ while these are invariant and approximately Gaussian (*gray lines*) for the latter. (C) The multifractal half-spectrum (i.e., $0 < q < 3$ in equation (1)) for the simple response task (*upper panel*) and the interval estimation task (*lower panel*) estimated by the coefficients of both MODWT (*black squares*) and CWT (*black circles*) with the ensemble of surrogates (*gray bars of* ±1 *standard deviation*).

The simple response task had a significantly larger multifractal spectrum width ($p <$ 0.01) for both the MODWT- and CWT-based computations (median 0.35 and 0.36, respectively) compared to the choice decision (median 0.11 and 0.19) and interval estimation

(median 0.06 and 0.09) tasks (see Figure 6). Furthermore, all of the 36 response series had an inhomogeneous variance unequal to independent, Gaussian-distributed MODWT coefficients according to the *D*-statistics ($p < 0.05$, see Eq. (A22) in the Appendix). This means that even though some of the response series have a multifractal spectrum width close to zero (see for example participants 3 and 5 in the short RSI interval estimation task in Figure 6C), the scale-dependent processes were nevertheless significantly less homogeneous compared to those of monofractal pink noise, as exemplified in the lower panel in Figure 3A. To summarize, re-analyzing Wagenmakers et al.'s (2004) data set using the MODWT and CWT indicated that a large portion of the response series is influenced by intermittent dynamics that are induced by interactions between their multiple time scales. The significant differences between the multifractal spectrum widths of the response series and their ensemble of surrogates (see Figure 6A-C) indicated that these interactions are not identified by the non-Gaussian probability density function or the $1/f^{\alpha}$ power law of the response series.

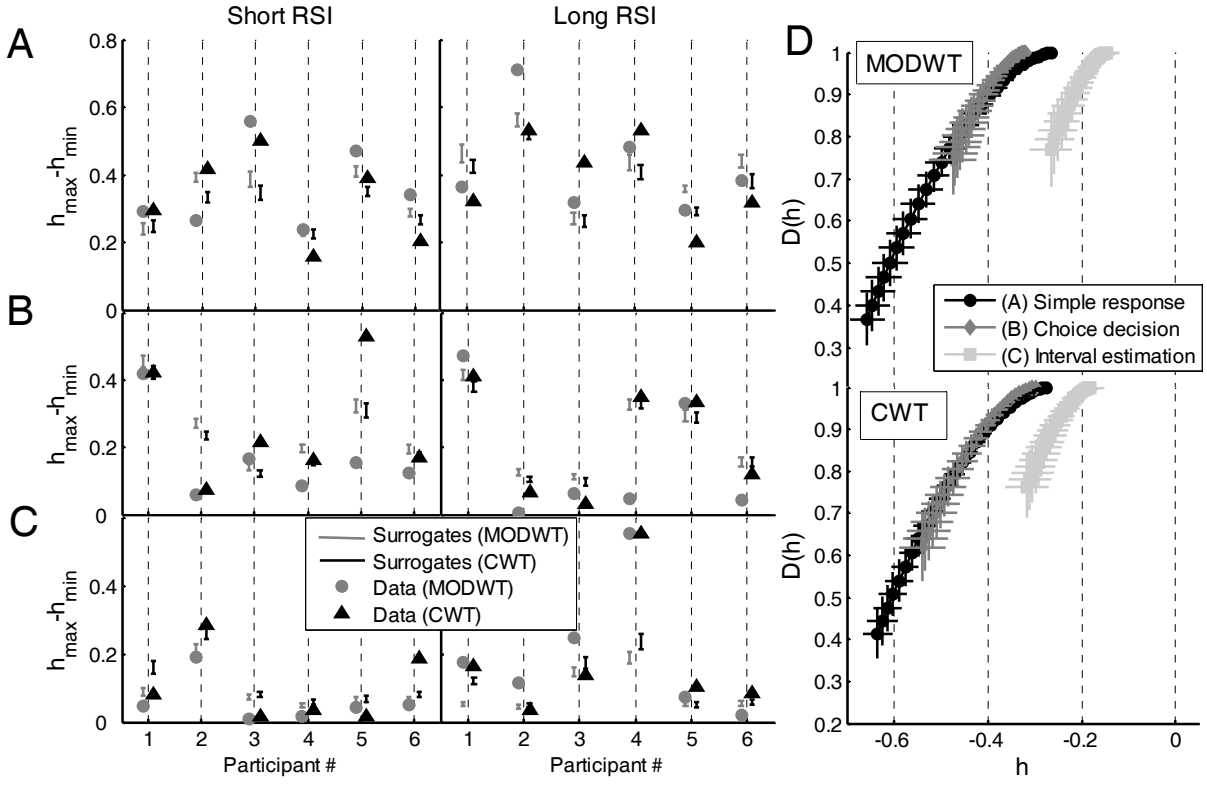

Figure 6: (A) The multifractal spectrum width $h_{max} - h_{min}$ for each participant estimated by both MODWT (*gray circles*) and CWT (*black triangles*) coefficients in a simple response task with short (*left panel*) and long (*right panel*) RSI. The circles with bars are the confidence intervals of $h_{max} - h_{min}$ for the surrogates estimated by MODWT (*gray bars*) and CWT (*black bars*) coefficients. (B) The same as in (A) for the choice decision task. (C) The same as in (A) for the interval estimation task. (D) The standard error intervals for the multifractal half-spectrum (i.e., $0 < q < 3$ in equation (1)) for simple response (*black*), choice decision (*gray*) and interval estimation (*light gray*) tasks estimated by both MODWT (*upper panel*) and CWT (*lower panel*) coefficients.

Data set 2: Van Orden et al.'s (2003) data set consists of 10 and 20 response time series of a simple and a word naming response task, respectively. In contrast to data set 1, the simple and word naming response task were between-subject manipulations. In the simple response task, the participants were responding as fast as possible to visual stimuli (+++) by an oral response \ta\ collected by a voice key. The response to stimulus interval was 415 ms. In the word naming response task, the oral response was reading out loud a visually displayed word of four or five letters, where the response to stimulus interval was 629 ms. After pre-processing the data in which values more than 3 standard deviations from the mean were eliminated, each response time series contained 1024 samples. The eliminated values were mainly artifacts of the voice key (cf. Van Orden et al., 2003).

Multiplicative interactions in data set 2: The response series of the simple response task showed periods of small and large variability just like the same task in data set 1. These periods were more distinct for the simple response task compared to the word naming task, as indicated by a less homogeneous wavelet variance when $\Delta t \rightarrow 0$ for the simple response task. Subsequently, this difference was quantified by the multifractal spectrum width $h_{max} - h_{min}$. There was a non-significant trend ($p = 0.068$) for a larger spectrum width for the simple response task (median 0.31) compared to the word naming response task (median 0.16) when the multifractal spectrum computation was based on the MODWT coefficients (see upper

panel in Figure 7B), while the difference was significant ($p = 0.04$) when the same computation was based on the CWT coefficients (median 0.34 vs 0.12) (see lower panel in Figure 7B). The individual multifractal spectrum widths $h_{max} - h_{min}$ together with the 95% confidence interval of the 30 ensembles is depicted in Figure 7A. As for data set 1, the *D*-statistics indicated that all of the 30 response series had an inhomogeneous wavelet variance ($p < 0.05$) different from the homogeneous variance of monofractal pink noise (see lower panel of Figure 3A). To summarize, re-analyzing Van Orden et al.'s (2003) data set using the MODWT and CWT indicated that, similar to data set 1, the response series are influenced by intermittent dynamics induced by interactions between their multiple time scales. Equivalent to data set 1, the significant difference between the multifractal spectrum width of the response series and the ensemble of surrogates ($p < 0.05$) indicated that these interactions cannot be identified by the non-Gaussian distribution or the $1/f^{\alpha}$ power law of the response series alone.

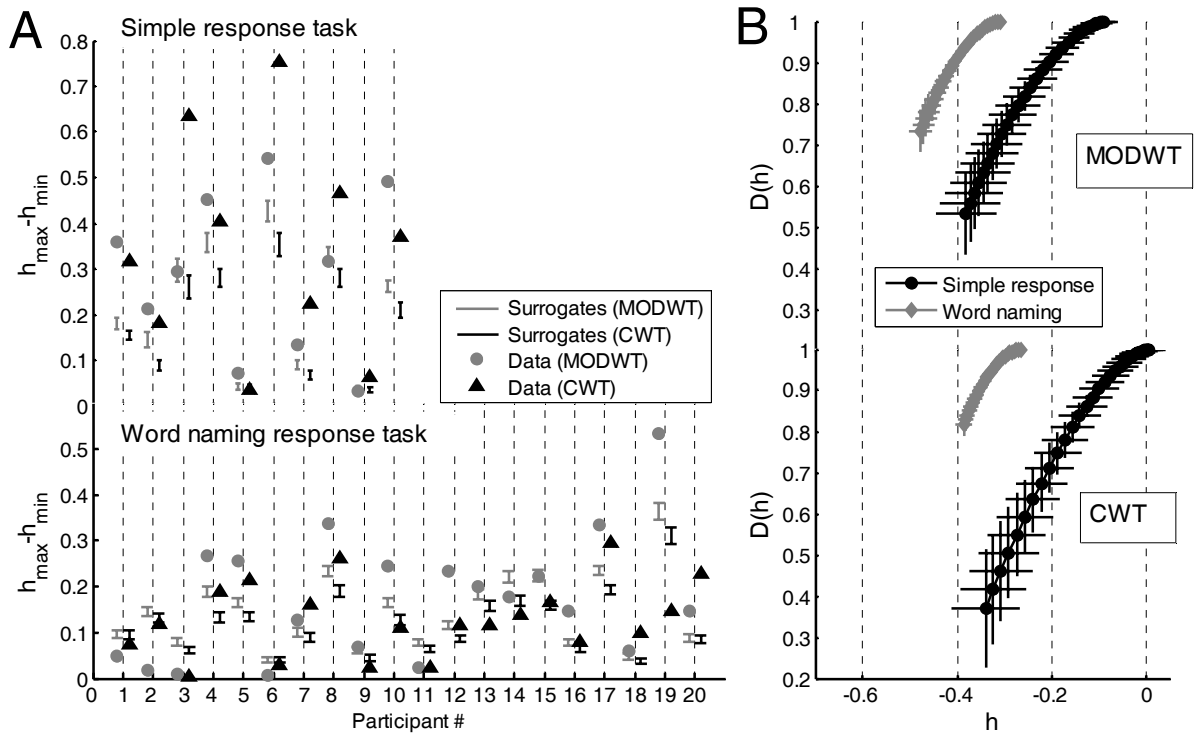

Figure 7: (A) The multifractal spectrum width $h_{max} - h_{min}$ for each participant estimated by both MODWT (*gray circles*) and CWT (*black triangles*) coefficients for the simple response (*upper panel*) and word naming (*lower panel*) tasks. The small circles and triangles with bars represent the confidence intervals of $h_{max} - h_{min}$ for the surrogates estimated by wavelet coefficients of MODWT (*gray bars*) and CWT (*black bars*). (B) The standard error intervals for the multifractal half-spectrum (i.e., $0 < q < 3$ in equation (1)) for simple response (*black*) and word naming (*gray*) tasks estimated by both MODWT (*upper panel*) and CWT (*lower panel*) coefficients.

Discussion: In the present re-analysis of the data sets of Wagenmakers et al. (2004) and Van Orden et al. (2003), the strongest influence of multiplicative interactions (i.e., multifractal spectrum width) was present in the simple response tasks of both data sets. This might be due to their common task instruction "respond as fast as possible to the stimulus". This instruction leads to consistent laminar periods with fast response times and little variability, while the intermittent bursts are skewed towards slow response times where the burst size is constrained by the upper time limit set by the experiment. Although this task has no ambiguity in either stimulus, response or instruction, its simplicity nevertheless leads to a larger difference between laminar periods of fast response times and intermittent periods of slow response times, in which the participants' attention to the stimulus or commitment to the experiment is waning. Furthermore, a large increase in response times is likely to induce a subsequent decrease in order to stay within the time limits of the experiment. Consequently, an intermittent zigzag pattern reflects a relationship between the width of the local probability density function and the local regularity (i.e., local *h* exponent) of the response series that are both implicit to a multifractal response pattern (see Figure A2 in the Appendix for the mathematical details).

In the interval estimation task, the internal cognitive representation of 1 second defines the performance variability (e.g., Gilden, 2001; Gilden et al., 1995; Wing & Kristofferson, 1973). The present re-analysis shows that this representation yields a decrease in the

multifractal spectrum width and, thus, less pronounced intermittent periods of large response time variability. An interesting difference between the instructions of the simple response task and the interval estimation task was that the latter contained a specification of the response duration "1 second". This specification may have decreased the influence of intermittent bursts of large variability by the overriding influence of the time metrics set by the experimental setup. Thus, there is less probability of sudden large increases in the time estimation and, consequently, a less pronounced irregular zigzag pattern seen in the interval estimation task. This difference is confirmed by stronger long-range correlations (i.e., more regularity) in the interval estimation task compared to the simple response task (Wagenmakers et al., 2004). Even though some of the response series in the interval estimation task were approximately monofractal (see lower panel of Figure 5C), the distribution of the wavelet coefficients was nevertheless inhomogeneous (see lower panel in Figure 5A). This indicates that the multiplicative interaction between temporal scales was not scale invariant and that some of the response series in the interval estimation task were neither multifractal nor monofractal (i.e., $1/f^{\alpha}$ noise). This point is discussed further in the third concluding remark at the end of the Appendix.

It has previously been suggested that both choice decision tasks and word naming tasks increase the memory work load of the cognitive system. Clayton and Frey (1997), for example, reported that regularity decreased towards uncorrelated fluctuation of the response series when the number of choices increased. This finding was later replicated by Ward (2002). Van Orden et al. (2003) showed that the response time fluctuation in word naming response tasks has a less correlated structure compared to the simple response task, whereas Wagenmakers et al. (2004) did not find such differences in the $1/f^{\alpha}$ power law between the simple response task and the choice decision task. The present results suggest that an increase in memory workload suppresses the waning of attention and thereby the coordination between

the multiple time scales of the response series. This suppression leads to a decrease in the multifractal spectrum width for both the choice decision and the word naming tasks compared to the simple response task. The suppression might have been caused by the duality of the oral instruction to "respond as fast as possible to the stimuli without error", resulting in a speed-accuracy trade-off between "respond as fast as possible" and "respond without error" to the stimuli. The addition of an accuracy instruction increased the variability in the laminar periods in the response series compared to the simple response task and, consequently, decreased the difference between the laminar and intermittent periods (i.e., a decrease in the multifractal spectrum width). This suggestion is supported by a less pronounced right tail of the non-Gaussian probability density function of the choice decision task compared to the simple response task in data set 1.

To summarize, the emergent periods of intermittent variability in both data sets were shown to originate from multiplicative interactions, as indicated by the significant difference between the multifractal spectrum width of the response series and their surrogates. The influence of these interactions was shown to be dependent on the task constraints, with the simple response task in both data sets displaying the most pronounced multiplicative interaction. These results indicate that there is a major influence of interactions across multiple time scales in cognitive performance, and illustrate the limitations of using the $1/f^{\alpha}$ power law to quantify interaction-dominant dynamics in cognitive performance.

Component- versus interaction-dominant models of cognitive performance

The section above provided quantitative support for the presence of multiplicative interactions between temporal scales in cognitive tasks. These interactions have previously been equated to the omnipresence of $1/f^{\alpha}$ fluctuations in cognitive performance (Kello et al.,

2007, 2008; Van Orden et al., 2002, 2003, 2005). As illustrated in the present paper, there is a fundamental deficit in this view because α and related exponents are blind to the presence of multiplicative interactions between scales (see the Appendix for the mathematical details of this claim). In other words, $1/f^{\alpha}$ fluctuation in cognitive performance can be caused by both component-dominant dynamics (Wagenmakers et al., 2004, 2005) and interaction-dominant dynamics (Kello et al., 2007, 2008; Van Orden et al., 2002, 2003, 2005). In this section, we will test the ability of two frequently used component-dominant models and the presently introduced multiplicative cascading process to reproduce the multiplicative interactions between temporal scales in the response series of data sets 1 and 2.

Response series = $1/f^{\alpha}$ fluctuation + white noise: The literature on cognitive dynamical systems has suggested that cognitive performance can be described as a generic superposition of $1/f^{\alpha}$ fluctuation and white noise, leading to a flattening of the log-Fourier spectrum at high frequencies (e.g., Gilden, 2001; Wagenmakers et al., 2004; Ward, 2002). This suggestion was first introduced by Gilden et al. (1995) for an interval estimation task, in which the $1/f^{\alpha}$ fluctuation was considered to be the generic property of the cognitive system while the (differentiated) white noise was caused by motor error corrections (e.g., Wing & Kristofferson, 1973) or priming effects (cf. Gilden, 2001). To test the hypothesis that cognitive performance can be exclusively defined by this model, 1000 simulated series were generated with a Fourier spectrum identical to each response series. This generation was obtained by randomizing the phases of the fast Fourier transformation but preserving the ordering of the amplitude. This resulted in a Fourier spectrum identical to the original response series and therefore a perfectly fitted *$1/f^{\alpha}$ fluctuation + white noise* model as used in the studies cited above. The simulated series were then decomposed by the MODWT and the *D*-statistics was employed for the scales Δt = 2, 4, 8, 16, and 32 trials to compare the wavelet

variances. In addition, a CWT-based estimation of the multifractal spectrum width ($h_{max} - h_{min}$) was computed for each simulated series and compared to the results of the response series of datasets 1 and 2.

Starting with the inhomogeneous wavelet variance, the *$1/f^{\alpha}$ fluctuation + white noise* simulated series were able to replicate this for only 1 of the 12 response series in the interval estimation task (participant 3, short RSI) and for none of the response series in the choice decision and simple response tasks of data set 1 ($p < 0.05$, see Eq. (A22) in the Appendix). For data set 2, the simulated series were able to replicate only 2 out of 10 response series in the simple response task (participants 5 and 9) and 4 out of 20 response series in the word naming task (participants 1, 7, 12, and 13). The inability to replicate inhomogeneous wavelet variance was most apparent for the smallest temporal scales $\Delta t = 2$, 4, and 8 trials, that are assumed to contain the priming effects or motor error correction terms (cf. Gilden, 2001; Gilden et al. 1995; Thornton & Gilden, 2005).

As for the mean multifractal spectrum widths, Figure 8 shows that these were close to zero for all simulated series, indicating that the *$1/f^{\alpha}$ fluctuation + white noise* model is not able to replicate the multiplicative interactions that are present in the response series. In the simple response task of data set 1, all simulated series had significantly narrower multifractal spectrum widths compared to the original response series ($p < 0.05$). In the choice decision task, 3 out of 12 response series (participant 2, short RSI, and participants 2 and 3, long RSI) had spectrum widths equal to the model, while this was the case for 5 out of 12 response series in the interval estimation task (participants 1, 3, 4, and 5, short RSI, and participant 2, long RSI). In dataset 2, 2 out of 10 response series in the simple response task (participant 5 and 9) and 5 out of 20 response series in the word naming task (participants 1, 3, 6, 9, and 11) had equal multifractal spectrum widths.

Combining both tests, only 4 out of 66 response series had both equal homogeneous wavelet variance and equal multifractal spectrum width as the *$1/f^{\alpha}$ fluctuation + white noise* model, indicating that this model is unable to replicate multiplicative interactions between the temporal scales in the response series of several cognitive tasks.

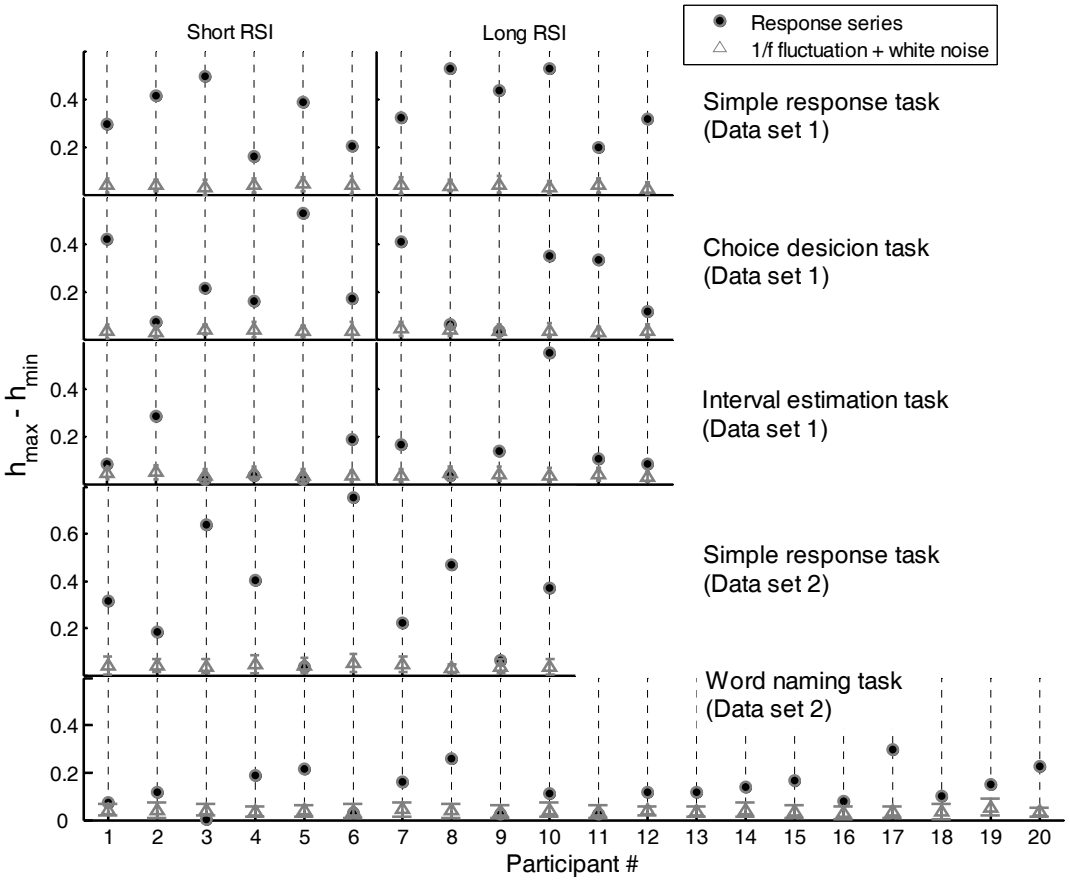

Figure 8: The multifractal spectrum width $h_{\max} - h_{\min}$ for the response series (*black dots*) in the simple response, choice decision, and interval estimation tasks of dataset 1 with short and long RSI, and in the simple response and word naming tasks of dataset 2. The mean (*gray triangles*) and ± 1 standard deviation is displayed for 1000 simulated series of the superposition of $1/f^{\alpha}$ fluctuation and white noise.

Response series = $AR_{\Delta t=100}+AR_{\Delta t=10}+AR_{\Delta t=1}$ + *white noise*: The $1/f^{\alpha}$ fluctuation in the model in the previous section can be further decomposed into an aggregated sum of autoregressive (AR) processes yielding *$1/f^{\alpha}$ fluctuation* = $AR_{\Delta t=100}+AR_{\Delta t=10}+AR_{\Delta t=1}$, where the subscripts are hypothesized to define the temporal scales (Δt) for the consciousness, sub-consciousness, and

unconsciousness processes, respectively[3]. This aggregated AR model was decomposed into wavelet coefficients at scales Δt = 2, 4, 8, 16, and 32 trials before the *D*-statistics were applied.

Starting again with the inhomogeneous wavelet variance in data set 1, only 1 out of 12 response series in the interval estimation task (participant 3, short RSI) and none of the response series in the simple response and choice decision tasks had equal inhomogeneous wavelet variance as the aggregated AR model ($p < 0.05$, see Eq. (A22) in the Appendix). In data set 2, this was the case for 2 out of 10 response series in the simple response task (participants 5 and 9) and 5 out of 20 response series in the word naming response task (participants 1, 2, 12, 13, and 18). The difference between the distribution of the wavelet coefficients of the models and the response series was largest for the three smallest temporal scales Δt = 2, 4, and 8 trials, where the presence of interaction-dominant dynamics was more pronounced.

With respect to the multifractal spectrum widths in data set 1, the aggregated AR model was not able to reproduce the width of any of the 12 response series in the simple response task ($p < 0.05$), while the width was replicated for 6 out of 12 response series in the choice decision task (participants 2, 4, and 6, short RSI, and participants 2, 3, and 6, long RSI) and 6 out of 12 response series in the interval estimation task (participants 1, 3, 4, and 5, short RSI, and participants 5 and 6, long RSI). In data set 2, the aggregated autoregressive model was able to reproduce the multifractal spectrum widths for 2 out of 10 response series in the simple response task (participants 5 and 9), and 7 out of 20 response series in the word naming task (participants 1, 2, 3, 6, 9, 11, and 18). Similar to the *fluctuation + white noise* model in Figure 8, the aggregated AR model was unable to replicate the multifractal structure of the response series.

[3] See Chapter 16 in Ward (2002) for the formal definition of this model.

According to both tests combined, only 5 out of 66 response series in data set 1 and 2 had equal homogenous wavelet coefficients and multifractal spectrum widths as the aggregated AR model. In summary, both $1/f^{\alpha}$ *fluctuation + white noise* and the aggregated AR model were unable to replicate multiplicative interactions between temporal scales in the response series of several cognitive tasks.

Response series as a multiplicative cascading process: The multiplicative cascading process illustrated in the upper panels of Figure 3 (and in Figures A1-A3 in the Appendix) is a multiplicative generalization of the additive models tested above. This means that we are moving from the component-dominant models above where the response series is assumed to be decomposable into independent time scales, to an interaction-dominant model where the time scales are interacting. The parameters of the multiplicative cascading process were the center tendency and width $h_{\max} - h_{\min}$ of the multifractal spectrum defined by the MODWT- and CWT-based estimations of the response series (see the Appendix for further mathematical details). The multiplicative cascading process was then decomposed into wavelet coefficients at scales $\Delta t = 2$, 4, 8, 16, and 32 trials before the *D*-statistics were applied. As the multifractal spectrum width is one of the parameters of the multiplicative cascading process, the spectrum widths were not compared to the response series.

The inhomogeneous wavelet variance was replicated by the multiplicative cascading process in 11 out of 12 response series in the simple response task (all except participant 1, long RSI), in 10 out of 12 response series in the choice decision task (all except participants 2 and 6, long RSI) and in 9 out of 12 response series in the interval estimation task (all except participants 3, 4, and 5, short RSI) of data set 1 ($p < 0.05$, see Eq. (A22) in the Appendix). In data set 2, the inhomogeneous wavelet variance was replicated in 9 out of 10 response series in the simple response task (all except participant 7), and in 18 out of 20 response series in the

word naming response task (all except participants 11 and 14). The multifractal structure of the multiplicative cascading process was able to replicate the intermittent periods of large wavelet variance in the response series especially for the three smallest temporal scales Δt = 2, 4, and 8 trials.

All in all, the multiplicative cascade process was able to replicate the scale-dependent variance in 57 out of 66 response series, indicating that it is a more suitable model of cognitive performance than the component-dominant models above. As illustrated in the upper panel of Figure 3B, the multiplicative cascading process is able to induce heavy tails in the wavelet coefficients especially at the smallest temporal scales Δt = 2, 4, and 8 trials, where the component-dominant models break down.

Discussion: The present paper has introduced an interaction-dominant model called a multiplicative cascading process for modeling the interactions across the multiple time scales of cognitive performance. The mathematical implication of the presence of multiplicative interactions in response series is that the fundamental assumption of the existence of mutually independent time scales breaks down. This means that the fundamental assumption of independent oscillations of the Fourier decomposition is violated, as are the corresponding labels of encapsulated cognitive constructs as independent levels of mental sets or consciousness (e.g., Gilden, 2001; Ward, 2002). Furthermore, the present results suggest that the white noise flattening of the Fourier spectrum is a consequence of interactions between the multiple time scales of the cognitive system rather than of superimposed motor error corrections or priming effects as previously suggested (Gilden, 2001; Wing & Kristofferson, 1973). The intermittency of the multiplicative cascading process induces transient periods of large response variability that have an irregular structure, i.e., a zigzag pattern with large amplitude and high frequency. In response series of finite size, these intermittent periods will

induce a flattening of the spectrum that is dependent on the width of the multifractal spectrum. This relationship was confirmed in both data set 1 and data set 2, with the simple response task having the most pronounced flattening at higher frequencies and the largest multifractal spectrum width. In addition, superimposed white noise on $1/f^{\alpha}$ fluctuation (or aggregated autoregressive processes) is approximately Gaussian distributed while the distributions of the response series have a heavy right tail that originates from the intermittent periods of large performance variability. Finally, the replication of the Fourier spectrum leads to homogenous wavelet variance at all temporal scales in the *$1/f^{\alpha}$ fluctuation + white noise* model, which was seen in only 4 of the 66 response series. In contrast to the component-dominant models, the present model of human cognition as a multiplicative cascading process defines the flattening region in the Fourier spectrum as part of the integrated whole of the cognitive system rather than as superimposed priming effects (e.g., Gilden, 2001) or motor error corrections (e.g., Gilden et al., 1995; Wing & Kristoffersen, 1973) that can be filtered out or subtracted from the cognitive dynamics. In summary, our results indicate that the transient, intermittent, incoherent and emergent behavior of the cognitive system results from the interactions between multiple time scales rather than from a superposition of encapsulated and non-interacting cognitive components.

Interaction-dominant dynamics in the human nervous system

The current application of multifractal analyses and corresponding multiplicative cascading processes to response series provides support for the interaction-dominant perspective on human cognition as a coherent whole characterized by interacting time scales. An alternative theoretical framework to capture interaction-dominant dynamics was recently suggested by Van Orden et al. (2003, 2005) and later Kello et al. (2007) and Holden et al.

(2009). Within this framework, $1/f^{\alpha}$ power laws and non-Gaussian probability density functions in response series are hypothesized to be common features of the human nervous system and behavior in a so-called self-organized critical state (Bak, 1996; Bak, Tang, & Wiesenfeld, 1987; Jensen, 1998). A self-organized critical system is driven by external injections of energy, mass, or information that is subsequently dissipated according to local interaction principles between the components of the system. In a critical state, the dissipation of energy, mass, or information is not constrained to the local sites of neighboring components but is present on all spatial scales. So far, this interaction-dominant framework has not quantified how this state of the human nervous system and behavior can be linked to the interactions between the temporal scales of cognitive function (e.g., Wagenmakers, 2005). In the physics literature, however, several models of self-organized criticality of the nervous system have recently been suggested, such as self-organized branching models (Beggs & Plenz, 2003; Juanico, Monterola, & Saloma, 2007; Lauritsen, Zapperi, & Stanley, 1996; Poil, van Ooyen, & Linkenkaer-Hansen, 2008; Zapperi, Lauritsen, & Stanley, 1995) and self-organized integrate-and-fire models (da Silva, Papa, & de Souza, 1998; Kinouchi, & Copelli, 2006; Levina, Herrmann, & Geisel, 2007; Usher, Stemmler, & Olami, 1995). Common for these models is a local threshold dynamics between adjacent neurons that leads to a dissipation of external or afferent stimuli across multiple spatial scales of the nervous system. When the nervous system is in a critical state, the dissipation is intermittent and consists of both local and global conduction paths of neural activity for any given stimulus. This intermittent spatial dissipation is analogous to the intermittent response time variability seen in the multiplicative cascading process and defines the sensitivity and adaptability of the cognitive system to external perturbations. Consequently, in both self-organized critical models and multiplicative cascading processes, global coordinated dynamics of the whole cognitive system emerge spontaneously through its local dynamics.

In this last part of the results, the multiplicative interactions between the temporal scales of cognitive performance are linked to the suggested interaction-dominant dynamics in the nervous system. This is obtained by comparing the multifractal spectrum widths $h_{max} - h_{min}$ of the output of a self-organized branching process developed by Zapperi and colleagues (1995), with the spectrum widths of the response series. We will then extend the multiplicative cascading process to the spatial domain of the human nervous system to illustrate the similarity with the self-organizing branching process.

Self-organizing branching process: The self-organizing branching process was defined in a neural network of 100 000 neurons where each neuron or site can be in a silent or potentiated state (Zapperi et al., 1995). When a neuron is stimulated, it converts from a silent to a potentiated state or from a potentiated to an active state. A neuron in the active state redistributes its stimulation to two randomly chosen nearest neighbors and then settles in a silent state. If a neighbor neuron is in a potentiated state, it also redistributes its stimulation so that conduction paths of action potentials are branching across the network. In contrast, if the neighbor neuron is in a silent state it is potentiated, but the conduction of the action potential to subsequent neighbors stops. The probability for these two conditions is given by the critical branching parameter p (Zapperi et al., 1995). If $p < 0.5$ there is a larger probability for the branching of the action potential to hit silent neurons and stop (see upper panel in Figure 9). In this sub-critical state, the number of active neurons will decrease as they redistribute their stimulation to their neighbors. The total number of neurons contributing to the conduction of action potentials will be small such that the neural interactions remain local in the nervous system (see upper panel in Figure 9). If $p > 0.5$ there is a larger probability for the branching of the action potential to hit potentiated neurons and branching further across the neural network. In this super-critical state, the number of active neurons will increase such that the

total number of active neurons will be high and the neural interactions will be global (see bottom panel in Figure 9). The critical state $p = 0.5$ is the borderline between these scenarios where the interactions are both local and global in the nervous system, leading to intermittent dissipation that makes the nervous system more adaptive to a given external stimulus. In other words, any given stimulation can give rise to both local and global neural interactions (see the middle panel of Figure 9).

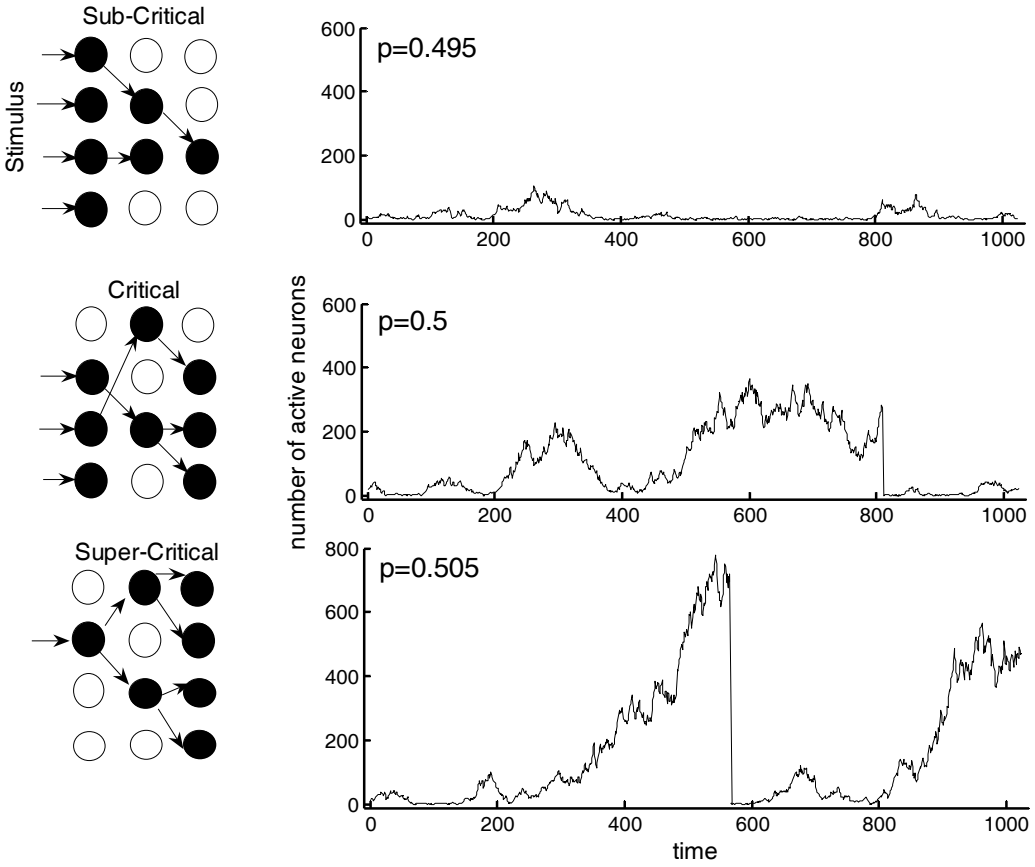

Figure 9: The time series of number of active neurons in a random network with a self-organized branching process for sub-critical (*upper panel*), critical (*middle panel*) and super-critical (*lower panel*) branching parameter p. (*Upper panels*) In the sub-critical state ($p = 0.495$), external stimulation leads to local activity only, as reflected in the small number of active neurons in the neural network. In this state, external stimuli are inhibited. (*Middle panels*) In the critical state ($p = 0.5$), there is both local and global activity yielding intermittent dissipation of external stimulation. In other words, external stimuli are both inhibited and propagated. This provides an intermittent mixture of both small and large numbers of active neurons in the neural network. (*Lower panel*) In the super-critical state ($p = 0.505$), there is mainly global activity apparent in

the build up of hills of a large number of active neurons as the external stimulation is branching across a large portion of the network. In this state, external stimuli are propagated. After the redistribution of external stimuli has branched across the network, the neural activity drops to the zero baseline before a new global branching is initiated.

We simulated 100 time series with 1024 data points of number of active neurons in the neural network for the self-organized branching process with the control parameter p in a close range of the critical point $p = 0.5$, ranging from the sub-critical state $p = 0.485$ to the super-critical state $p = 0.515$. Subsequently, we calculated the multifractal spectrum width $h_{max} - h_{min}$ for the synthesized time series where $h_{max} - h_{min}$ was validated by an ensemble of 30 surrogate series (see 'Validation of multiplicative interactions' in the method section).

The number of active neurons in the self-organizing branching process at each time instant shows an increase in intermittent structure going from a sub-critical to a super-critical state in the vicinity of $p = 0.5$. This change in structure is closely related to a sudden increase in the multifractal spectrum width around $p = 0.5$ where the process enters the super-critical domain (see upper panel of Figure 10). In the super-critical domain, there are mainly large, global conductions of neural activity reflecting the intermittent periods of global activity and, thus, large multifractal spectrum width. In contrast, in the sub-critical domain the activations are small and localized, causing more homogeneous variability in the activation and therefore a narrow multifractal spectrum width. Interestingly, when comparing the results of 100 synthesized series of the self-organized branching process for each parameter p, a larger standard deviation of the multifractal spectrum width was observed for the critical state $p = 0.5$ (see lower panel of Figure 10). Furthermore, the multifractal spectrum width of the 66 response series in data sets 1 and 2 were within 2 standard deviations of the critical state $p = 0.5$ (see lower panel of Figure 10). This indicates that in the critical state a more diverse range of neural activity appears, reflected as intermittent structure in the response series, that

provides the organism with the flexibility to adapt to changes in the environment. In summary, the present results provide quantitative support that the cognitive system might live in a close range around its critical point where it can adapt to small differences in external stimuli, which would not be possible in the sub-critical or super-critical domain alone.

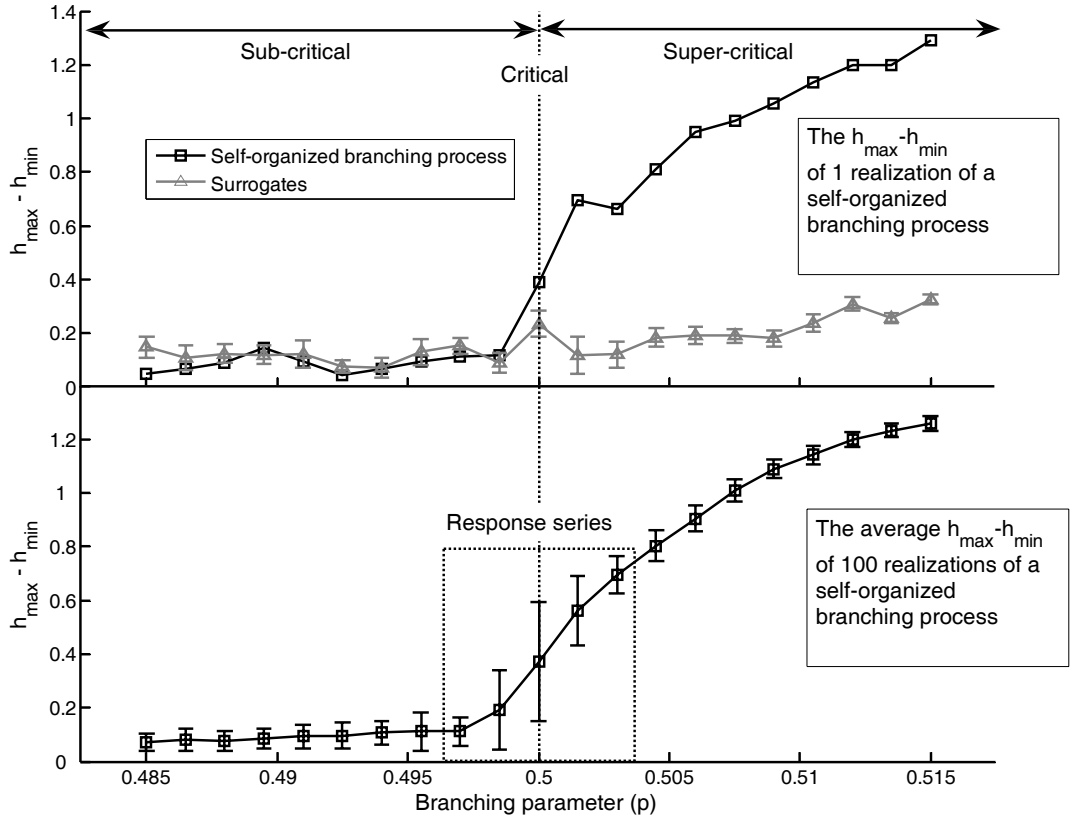

Figure 10: (*Upper panel*) The multifractal spectrum width $h_{\max} - h_{\min}$ for the time series of the number of active neurons in a self-organized branching process with the branching parameter between 0.485 and 0.515 (*black trace*). The activity pattern shifts from an approximately monofractal to a multifractal structure around the critical point $p = 0.5$. In the critical and super-critical state, the self-organized branching process has significant influence of multiplicative interactions across temporal scales as indicated by the significant difference with the ensemble of surrogates (*gray error bars*). (*Lower panel*) The standard deviation of the multifractal spectrum width $h_{\max} - h_{\min}$ for 100 realizations of a self-organized branching processes. The standard deviation is larger around the critical state $p = 0.5$ where the multifractal spectrum width of the response series lies within ±2 standard deviations of the critical state (indicated by the height of the box*)*.

Neural activity as a multiplicative cascading process: The intermittent dissipation of external stimulation of the self-organizing branching process implies an inhomogeneous distribution of neural activity as observed in fMRI recordings in rest and during cognitive tasks (e.g., Liu, Liao, Fang, Chu, & Tan, 2004; Menon, Luknowsky, & Gati, 1998; Richter, Ugurbil, Georgopoulos, & Kim, 1997). This inhomogeneous distribution can be modeled by extending a multiplicative cascading process to multiplicative interactions between spatial scales (Chainais, 2006). In this extension, the scale Δx is the diameter of a shrinking sphere centered at the spatial coordinate $\boldsymbol{x}$ within the neural network (see Figure 11) rather than the diameter Δt of the cone in Figure 1B. When the product of interaction multipliers within the shrinking sphere of Figure 11 is large, there is globally coordinated neural activity within this sub-volume of the nervous system where the activity spreads across multiple spatial scales. In contrast, if the cumulative product of multipliers within the shrinking sphere is small, there is a sub-volume of local neural activity. Figure 12, upper panel, represents the simulation of a multiplicative cascading process in three spatial dimensions that contains 125 000 sites. The blue to red color spectrum defines the level of activity, and the width of sheets the gradient spread of activity. The upper panel shows that interactions across multiple spatial scales form intermittent regions of high activity indicated by extended and interconnected red and yellow regions (i.e., global coordinated structures), and laminar regions of local small activity

defined by small blue sheets.

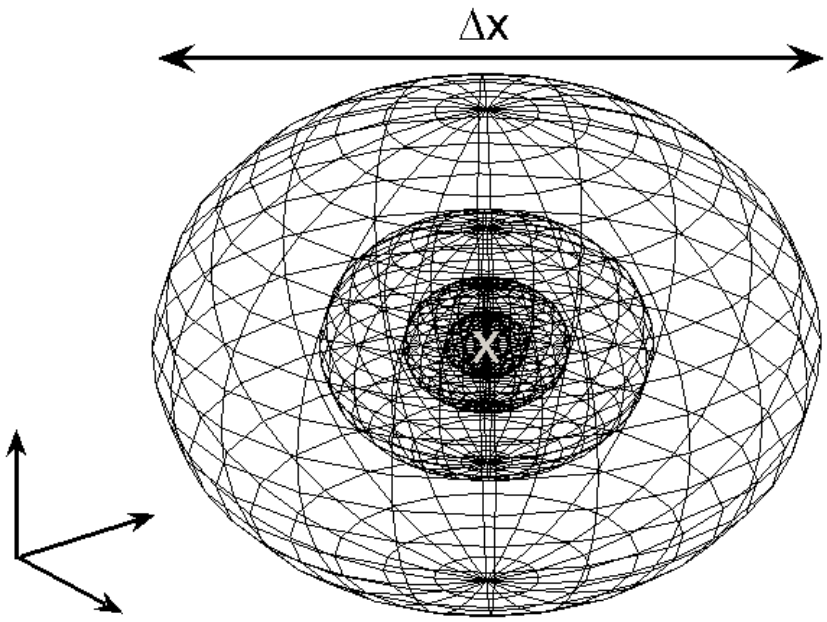

Figure 11: Construction of a three dimensional extension of a multiplicative cascading process, defined by extending the cone in Figure 1B to a shrinking sphere. The shrinking sphere defines the spatial scale Δx as its diameter, analogous to the temporal scale Δt for the cone in Figure 1B. This sphere is translated across the three spatial dimensions, with its center $\boldsymbol{x}$ (indicated by the gray 'x' in the center) being analogous to the tip t of the cone in Figure 1B.

Interaction-dominant dynamics in the nervous system

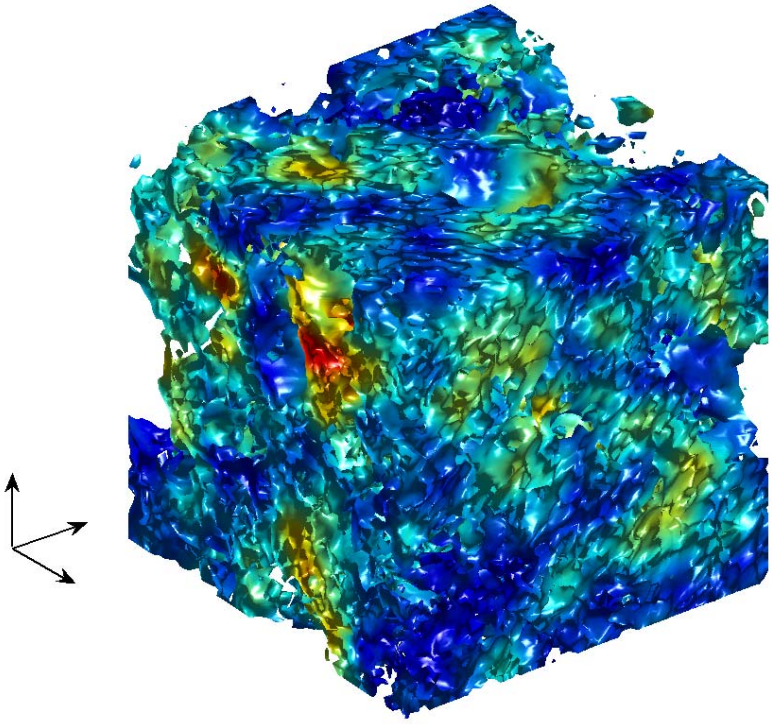

Component-dominant dynamics in the nervous system

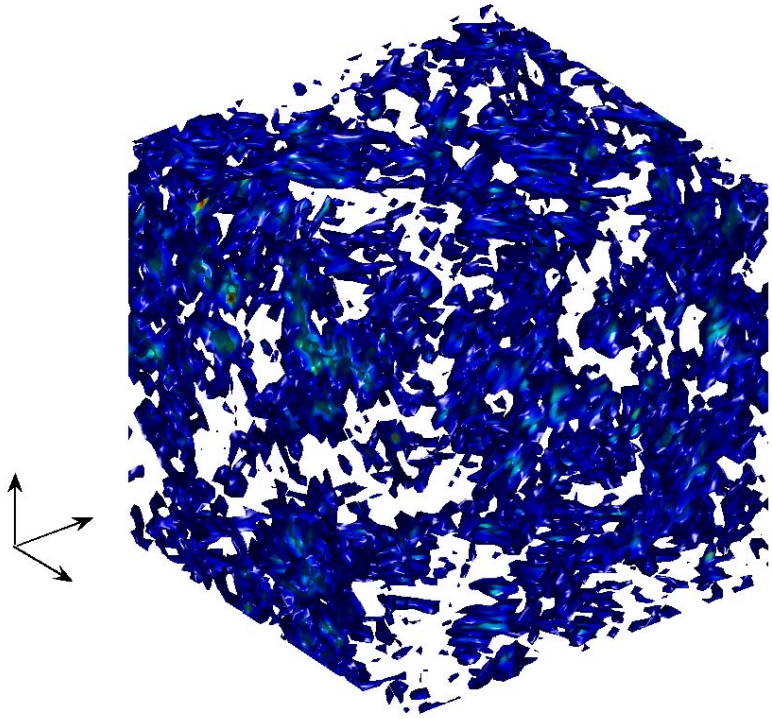

Figure 12: (*Upper panel*) A multiplicative cascading process of neural activation illustrating the presence of multiplicative interactions across spatial scales of the human nervous system. The extended red and yellow sheets illustrate the neural clusters with large and global activity, while the patchy blue sheets illustrate the clusters with little and local activity. A complex and intermittent structure of neural activation emerges from neural interaction and coordination across multiple spatial scales. (*Lower panel*) A surrogate generated by the iterated amplitude-adjusted three-dimensional Fourier transformation of the multiplicative cascading process in the upper panel. Although both the $1/f^{\alpha}$ scaling relation and non-Gaussian distribution of the neural activity are preserved, the multiplicative interactions between the spatial scales are eliminated. The lack of coordination and interaction between the spatial scales of the neural network generates small blue sheets of local activity similar to the sub-critical domain of the self-organized branching process in the upper panel of Figure 9.

By generating a surrogate of the multiplicative cascading process (see 'Validation of multiplicative interactions' in the method section) that replicates both the non-Gaussian distribution and monofractal structure (i.e., $1/f^{\alpha}$ power law), it is possible to illustrate the influence of neural interactions across spatial scales. The bottom panel in Figure 12 illustrates that when no interactions are present between spatial scales of the nervous system, only local neural activity is present (small blue sheets of activity across the entire network) without clusters of global coordinated activity as seen in the upper panel. In this monofractal case, no interactions across global ranges in the nervous system emerge, which is the equivalent to the sub-critical domain in the upper panel of Figure 10 of the self-organized branching process.

In summary, the present comparison of a self-organizing branching process and a multiplicative cascading process indicates that global coordinated neural activity can be generated by the intermittent dissipation of external stimulation across the multiple spatial scales of the nervous system. Thus, the self-organization of active neural clusters within the human nervous system and the self-assembly of intermittent variability seen in the response series may be closely related through interactions across multiple scales in both time and space.

Discussion: The present results indicate that multifractal fluctuations in the response series might be linked to multifractal neural activation within the human nervous system in close vicinity of its critical state. However, this comparison between interaction-dominant dynamics in response series and a self-organized branching process in the nervous system is based on modeling only, and physiological measurements of neural activation are necessary to validate the presence of intermittent distributed neural activity during cognitive tasks. Recent studies confirm that alpha oscillations in EEG and MEG recordings of the human cortex display intermittent periods of large amplitudes with similar pattern as the output of the self-organized branching process (Linkenkaer-Hansen, Nikouline, Palva, & Ilmoniemi, 2001; Linkenkaer-Hansen, Nikulin, Palva, Kaila, & Ilmoniemi, 2004; Poil et al., 2008). The present results on a self-organized branching process also indicate that neural activity in the nervous system and the behavioral output might be linked through their intermittent and multifractal structure. Thus, further studies are needed to investigate the correlation between the multifractal structure of the oscillation amplitudes in EEG and MEG and interactions across multiple time scales of cognitive performance.

Recently, a complex systems theory has been introduced in physics that compares and integrates multiplicative cascading processes and self-organized critical models (e.g., Bak, & Paczuski, 2005; Katsuragi et al.,, 2003; Sinha-Ray, de Agua, & Jensen, 2001; Sreenivasan, Bershadskii, & Niemela, 2004; Tebali, De Menech, & Stella, 1999; Uritsky, Paczuski, Davila, & Jones, 2007). Although this theory can distinguish multiplicative cascading processes and self-organized critical models in the limits of infinitely long time series (Boffetta, Carbone, Giuliani, Veltri, & Vulpiani, 1999), this distinction is not yet possible in the investigation of finite sized measurements, as in the case of human brain and behavior. Therefore, an integrated interaction-dominant theory of both self-organized criticality and multiplicative

cascading processes might be a promising way for future investigations of human cognition and behavior. Furthermore, several studies in solar physics show that self-organized criticality can develop a scale-free, fractal architecture of complex networks (Paczuski, & Hughes, 2004). Complex networks with scale-free, fractal structures are reported to be more robust to context-induced perturbations and have enhanced speed of energy and information propagation (Albert, Jeong, & Barabasi, 2000; Barabasi, & Albert, 1999; Song, Havlin, & Makse, 2006). A promising extension of the present study would be to apply these theories of complex networks to the architecture and functioning of the human brain.

Conclusion

The present study provided quantitative support for a paradigm shift towards interaction-dominant dynamics of human cognition by equating the latter with multiplicative interactions across the temporal scales of cognitive performance and the spatial scales of the human nervous system. The wavelet-based multifractal analysis was able to parameterize these multiplicative interactions in the performance of several cognitive tasks, caused by changes in attention to the stimulus or intention to comply with the experimental instructions. These multiplicative interactions between temporal scales in the response series fundamentally advance both what can be quantified and how to understand the basis of human behavior. The influence of the multiplicative interactions was quantified by the multifractal spectrum width, which in turn was shown to be dependent on the interrelation between the task instruction and the changes in attention to the stimulus or intention to comply. Furthermore, only the presently introduced multiplicative cascading process was able to model the intermittent fluctuations in the response series by incorporating the multiplicative interactions between temporal scales. Component-dominant models like '$1/f^{\alpha}$ fluctuation +

white noise' and 'aggregated AR processes' were unable to replicate the presence of multiplicative interactions, indicating that cognitive performance cannot be decomposed into independent cognitive categories like mental sets, level of consciousness, motor error corrections, or priming effects, as previously suggested in the literature (Gilden, 2001; Ward, 2002). The influence of the multiplicative interactions in the response series was shown to be closely related to the self-assembly of neural activity within the human nervous system, as defined by a self-organized branching process. The latter shared the same characteristics as a spatial extension of a multiplicative cascading process. These preliminary results illustrate a close relationship between the interactions across the temporal scales of cognitive performance and neural interactions across the spatial scales of the human nervous system. The present paper therefore points towards the possibility of a coherent theory for interaction-dominant dynamics in the human brain and behavior.

Acknowledgments

The authors express their sincere gratitude to Eric-Jan Wagenmakers, Simon Farrell, and Roger Ratcliff for making data set 1 available, to Guy C. Van Orden, John G. Holden, and Michael T. Turvey for making data set 2 available, and to Simon-Shlomo Poil for making the Matlab script for the self-organized branching process available. The algorithms used in this study were implemented in Matlab 7.1 using scripts from the following sources:

MODWT: http://www.atmos.washington.edu/~wmtsa/,

Weighted least square: http://www.cubinlab.ee.unimelb.edu.au/~darryl/,

Multiplicative cascading process: http://www.isima.fr/~chainais/PUB/software.html.

Iterated amplitude adjusted three dimensional Fourier transformation: http://www.meteo.uni-bonn.de/mitarbeiter/venema/themes/surrogates/iaaft/iaaft_download.html

References

Abry, P., Flandrin, P., Taqqu, M. S., & Veitch, D. (2000). Wavelets for the analysis, estimation, and synthesis of scaling data. In K. Park & W. Willinger (Eds.), *Self-similar network traffic and performance evaluation* (pp. 39-88). New York: Wiley.

Abry, P., Flandrin, P., Taqqu, M. S., & Veitch, D. (2002). Self-similarity and long-range dependence through the wavelet lens. In P. Doukhan, G. Oppenheim & M. S. Taqqu (Eds.), *Theory and applications of long-range dependence* (pp. 527-556). Boston: Birkhäuser.

Albert, A., Jeong, H., & Barabasi, A. (2000). Error and attack tolerance of complex networks. *Nature,* 406, 378-382.

Aldroubi, A., & Unser, M. (1996). *Wavelets in medicine and biology*. Boca Raton: CRC-Press.

Arneodo, A., Manneville, S., & Muzy, J. F. (1998). Towards log-normal statistics in high Reynolds number turbulence. *The European Physical Journal B*, 1, 129-140.

Ashkenazy, Y., Havlin, S., Ivanov, P. C., Peng, C. K., Frohlinde, V. S., & Stanley, H. E. (2003). Magnitude and sign scaling in power-law correlated time series. *Physica A*, 323, 19-41.

Bacry, E., Kozhemyak, A., & Muzy, J. F. (2008). Continuous cascade models for asset returns. *Journal of Economic Dynamics and Control*, 32(1), 156-199.

Bacry, E., & Muzy, J. F. (2003). Log-infinitely divisible multifractal processes. *Communication in Mathematical Physics*, 236, 449-475.

Bacry, E., Muzy, J. F., & Delour, J. (2001). Multifractal random walks. *Physical Review E*, 64, 026103-026106.

Bak, P. (1996). *How nature works: The science of self-organized criticality*. New York: Springer-Verlag.

Bak, P., & Paczuski, M. (2005). Luminous matter may arise from a turbulent plasma state of the early universe. *Physica A*, 348, 277-280.

Bak, P., Tang, C., & Wiesenfeld, K. (1987). Self-organized criticality: An explanation of 1/*f* noise. *Physical Review Letters,* 59, 381-384.

Barabasi, A.-L., & Albert, R., (1999). Emergence of scaling in random networks. *Science,* 286, 509-512.

Beggs, J. M., & Plenz, D. (2003). Neural avalance in neocortical circuits. *The Journal of Neuroscience*, 23 (35), 11167-11177.

Bloomfield, P. (1976). Complex demodulation. In P. Bloomfield (Ed.), *Fourier analysis of time series: An introduction* (pp. 118-150). New York: Wiley.

Boffetta, G., Carbone, V., Giuliani, P., Veltri, P., & Vulpiani, A. (1999). Power laws in solar flares: Self-organized criticality or turbulence? *Physical Review Letters*, 83 (22), 4662–4664.

Bollerslev, T., (1986). Generalized Autoregressive Conditional Heteroskedasticity. *Journal of Econometrics*, 31, 307-327.

Castaing, B., Gagne, Y., & Hopfinger, E. (1990). Velocity probability density functions of high Reynolds number turbulence. *Physica D*, 46, 177-200.

Chainais, P. (2006). Multidimensional infinite divisible cascades. Application to the modeling of intermittency in turbulence. *The European Physical Journal B*, 51(2), 229-243.

Chainais, P., Riedi, R., & Abry, P. (2005). On non-scale-invariant infinitely divisible cascades. *IEEE Transaction on Information Theory*, 51 (3), 1063-1083.

Chen, Y., Ding, M., & Kelso, J. A. S. (1997). Long-memory processes (1/*f* type) in human coordination. *Physical Review Letters,* 79, 4501-4504.

Chen, Y., Ding, M., & Kelso, J. A. S. (2001). Origins of time errors in human sensorimotor coordination. *Journal of Motor Behavior,* 33, 3–8.

Clayton, K., & Frey, B. (1997). Studies of mental "noise". *Nonlinear Dynamics, Psychology, and Life Sciences*, 1, 173-180.

da Silva, L., Papa, A. R. R., & de Souza, A. M. C. (1998). Criticality in a simple model for brain functioning. *Physics Letters A*, 242 (6), 343-348.

Daubechies, I. (1992). *Ten lectures on wavelets*. Philadelphia: SIAM.

Delignières, D., Lemoine, L., & Torre, K. (2004). Time intervals production in tapping and oscillatory motion. *Human Movement Science*, 23 (2), 87-103.

Delignières, D., Torre, K., & Lemoine, L. (2008). Fractal models for event-based and dynamical timers. *Acta Psychologica*, 127 (2), 382-397.

Ding, M., Chen, Y., & Kelso, J. A. S. (2002). Statistical analysis of timing errors. *Brain and Cognition*, 48 (1), 98-106.

Edelman, G. M. (1987). *Neural Darwinism: The theory of neuronal group selection*. New York: Basic Books.

Fang, F. (2006). Information of structures in galaxies distributions. *The Astrophysical Journal*, 644, 678-686.

Farrell, S., Wagenmakers, E. J., & Ratcliff, R. (2006). 1/*f* noise in human cognition: Is it ubiquitous, and what does it means? *Psychonomic, Bulletin & Review*, 13(4), 737-741.

Frank, T. D. (2004). Complete description of a generalized Ornstein–Uhlenbeck process related to the nonextensive Gaussian entropy. *Physica A*, 340, 251-256.

Gabor, D. (1946). Theory of Communication. *Journal of Institute for Electronics Engineers*, 93, 429-457.

Gilden, D. L. (1997). Fluctuations in the time required for elementary decision. *Psychological Science,* 8(4), 296-301.

Gilden, D. L. (2001). Cognitive emissions of 1/*f*-noise. *Psychological Review,* 108(1), 33–56.

Gilden, D. L., Thornton, T., & Mallon, M. W. (1995). 1/*f*-noise in human cognition. *Science,* 267, 1837-1839.

Goupillaud, P., Grossmann, A., & Morlet, J. (1984). Cycle-octave and related transforms in seismic signal analysis. *Geoexploration*, 23, 85−102.

Holden, J. G. (2002). Fractal characteristics of response time variability. *Ecological Psychology*, 14, 53-86.

Holden, J. G., Van Orden, G. C., & Turvey, M. T. (2009). Dispersion of response times reveals cognitive dynamics. *Psychological Review*, 116 (2), 318-342.

Huang, N. E., Shen, Z., Long, S. R., Wu, M. C., Shih, H. H., Zheng, Q., Yen, N.-C., Tung, C. C., & Liu, H. H. (1998). The empirical mode decomposition and the Hilbert spectrum for nonlinear and non-stationary time series analysis. *Proceedings of the Royal Society A*, 454, 903-995.

Hubbard, B. B. (1998). *The world according to wavelets: The story of mathematical technique in the making* (2th ed.). Natick: AK Peters Ltd.

Ihlen, E. A. I. (2009). A comparison of two Hilbert spectral analyses of heart rate variability. *Medical and Biological Engineering and Computing*, 47, 1035-1044.

Ivanov, P. C., Rosenblum, M. G., Peng, C.-K., Mietus, J., Havlin, S., Stanley, H. E. & Goldberger A. L. (1996). Scaling behavior of heartbeat intervals obtained by wavelet-based time series analysis. *Nature,* 383, 323-327.

Ivanov, P. C., Amaral, L. A. N., Goldberger, A. L., Havlin, S., Rosenblum, M. G., Struzik, Z. R., & Stanley, H. E. (1999). Multifractality in human heartbeat dynamics. *Nature,* 399, 461-465.

Jaffard, S., Lashermes, B., & Abry, P. (2006). Wavelet leaders in multifractal analysis. In T. Qian, M. I. Vai & Y. Xu, (Eds.), *Wavelet Analysis and Applications* (pp. 219–264). Basel: Birkhäuser Verlag.

Jensen, H. J. (1998). *Self-organized criticality*. Cambridge: Cambridge University Press.

Juanico, D. E., Monterola, C., & Saloma, C. (2007). Dissipative self-organized branching in a dynamic population. *Physical Review E*, 75 (4), 045105.

Kalisky, T., Ashkenazy, Y., & Havlin, S. (2005). Volatility of linear and nonlinear time series. *Physical Review E*, 72(1), 011913.

Kandel, E. R., Schwartz, J. H., Jessell, T. M. (2000). *Principles of neural science* (4th ed.). New York: McGraw-Hill.

Kantelhardt, J. W., Zschiegner, S. A., Koscielny-Bunde, E., Havlin, S., Bunde, A., & Stanley, H. E. (2002). Multifractal detrended fluctuation analysis of nonstationary time series. *Physica A*, 316, 87-114.

Katsuragi, H., Sugino, D., & Honjo, H. (2003). Scaling of impact fragmentation near the critical point. *Physical Review E*, 68(4), 046105.

Kavasseri, R. G., & Nagarajan, R. (2005). A multifractal description of wind speed records, *Chaos, Solitons & Fractals*, 24(1), 165-173.

Kello, C. T., Anderson, G. G., Holden, J. G., & Van Orden, G. C. (2008). The pervasiveness of 1/*f* scaling in speech reflects the metastable basis of cognition. *Cognitive Science*, 32, 1-15.

Kello, C. T., Beltz, B. C., Holden, J. G., & Van Orden, G. C. (2007). The emergent coordination of cognitive function. *Journal of Experimental Psychology: General*, 136, 551-568.

Kesten, H. (1973). Random difference equations and renewal theory for product of random matrices. *Acta Mathematica*, 131, 207-248.

Kinouchi, O., & Copelli, M. (2006). Optimal dynamical range of excitable networks at criticality. *Nature Physics*, 2, 348-352.

Lashermes, B., Abry, P., & Chainais, P. (2004). New insight in the estimation of scaling exponents. *International Journal of Wavelets and Multiresolution Information Processing*, 2 (4), 497-523.

Lauritsen, K. B., Zapperi, S., & Stanley, H. E. (1996). Self-organized branching processes: Avalanche models with dissipation. *Physical Review E*, 54(3), 2483-2488.

Lemoine, L., Torre, K., & Delignières, D. (2006). Testing for the presence of $1/f$ -noise in continuation tapping data. *Canadian Journal of Experimental Psychology,* 60 (4), 247-257.

Levina, A., Herrmann, J. M., & Geisel, T. (2007). Dynamical synapses causing self-organized criticality in neural networks. *Nature Physics*, 3, 857-860.

Lin, D. C. (2003). Robustness and perturbation in the modeled cascade heart rate variability. *Physical Review E*, 67, 031914.

Linkenkaer-Hansen, K., Nikouline, V. V., Palva, J. M., & Ilmoniemi, R. J. (2001). Long-range temporal correlations and scaling behaviour in human brain oscillations. *The Journal of Neuroscience,* 21(4), 1370-1377.

Linkenkaer-Hansen, K., Nikulin, V. V., Palva, J. M., Kaila, K., & Ilmoniemi, R. J. (2004). Stimulus-induced change in long-range temporal correlations and scaling behaviour of sensorimotor oscillations. *European Journal of Neuroscience,* 19, 203-218.

Liu, H. L., Liao, W.-T., Fang, S.-Y., Chu, T.-C., & Tan, L. H. (2004). Correlation between temporal response of fMRI and fast reaction time in a language task. *Magnetic Resonance Imaging*, 22 (4), 451-455.

Mallat, S. (1989). A theory for multi-resolution signal decomposition: The wavelet representation. *IEEE-TPAMI*, 11, 674-693.

Mallat, S. (1999*). A wavelet tour in signal processing* (2th ed.). San Diego: Academic Press.

Mandelbrot, B. B. (1974). Intermitttent turbulence in self-similar cascades: divergence of high moments and dimension of the carrier. *Journal of Fluid Mechanics,* 62, 331-358.

Mandelbrot, B. B. (1997). *Fractals and scaling in finance*. New York: Springer-Verlag.

Mandelbrot, B. B, & van Ness, J. W. (1968). Fractional Brownian motions, fractional noises and applications. S*IAM Review*, 10, 422-437.

Manimaran, P., Panigrahi, P. K., & Parikh, J. C. (2005). Wavelet analysis and scaling properties of time series. *Physical Review E*, 72 (4), 046120-046124.

Menon, R. S., Luknowsky, D. C., & Gati, J. S. (1998). Mental chronometry using latency-resolved functional MRI. *Proceedings of the National Academy of Sciences*, 95, 10902-10907.

Muzy J. F., & Bacry, E. (2002). Multifractal stationary random measures and multifractal random walks with log-infinitely divisible scaling laws. *Physical Review E*, 66(5), 056121.

Muzy, J. F., Bacry, E., & Arneodo, A. (1991). Wavelets and multifractal formalism for singular signals: Application to turbulence data. *Physical Review Letter,* 67(25), 3515-3518.

Muzy, J. F., Bacry, E., & Arneodo, A. (1993). Multifractal formalism for fractal signals: The structure-function approach versus the wavelet-transform modulus-maxima method. *Physical Review E,* 47(2), 875-884.

Muzy, J. F., Bacry, E., & Arneodo, A. (1994), The multifractal formalism revisited with wavelets. *International Journal of Bifurcation and Chaos*, 4, 245-302.

Muzy J. F., Bacry, E., & Kozhemyak, A. (2006). Extreme values and fat tails of multifractal fluctuations. *Physical Review E*, 73(6), 066114.

Olhede, S., & Walden, A. T. (2005) A generalized demodulation approach to time-frequency projections for multicomponent signal. *Proceedings of the Royal Society A*, 461, 2159-2179.

Paczuski, M., & Hughes, D. (2004). A heavenly example of scale-free networks and self-organized criticality. *Physica A,* 342, 158-163.

Percival, D. B., & Walden, A. T. (2000). *Wavelet methods for time series analysis*. Cambridge: Cambridge University Press.

Poil, S.-S., van Ooyen, A., & Linkenkaer-Hansen, K. (2008). Avalanche dynamics of human brain oscillations: relation to critical branching processes and temporal correlations. *Human Brain Mapping,* 29, 770-777.

Prasad, L., & Lyengar, S. S. (1997). *Wavelet analysis with applications to image processing*. Boca Raton: CRC-Press.

Pressing, J., (1999). Sources of 1/*f*-noise effects in human cognition and performance. *Paideusis*, 2, 43-59.

Pressing, J., & Jolley-Rogers, G. (1997). Spectral properties of human cognition and skill. *Biological Cybernetics*, 76(5), 339-347.

Richter, W., Ugurbil, K., Georgopoulos, A., & Kim, S.-G. (1997). Time-resolved fMRI of mental rotation. *Neuroreport*, 8, 3697-3702.

Riedi, R. H. (2002). Multifractal processes. In P. Doukhan, G. Oppenheim, & M. S. Taqqu (Eds.), *Theory and applications of long-range dependence* (pp. 625-716), Boston: Birkhäuser.

Scafetta, N., Griffin, L., & West, B. J. (2003). Hölder exponent spectra for human gait. *Physica A*, 328, 561-583.

Schreiber, T., & Schmitz, A. (1996). Improved surrogate data for nonlinearity tests. *Physical Review Letters*, 77, 635–638.

Sinha-Ray, P., de Agua, L. B., & Jensen, H. J. (2001). Threshold dynamics, multifractality and universal fluctuation in the SOC forest-fire: facets of an auto-ignition model. *Physica D*, 157 (3), 186-196.

Song, C., Havlin, S., & Makse, H. A. (2006). Orgins of fractality in the growth of complex networks. *Nature Physics,* 2, 275-281.

Sornette, D. (2004). *Critical phenomena in natural sciences: Chaos, fractals, self-organization and disorder: Concepts and tools (Springer Series in Synergetics)*. New York: Springer.

Sornette, D., & Ouillon, G. (2005). Multifractal scaling of thermally activated rupture processes, *Physical Review Letters*, 94, 038501.

Sreenivasan, K. R., Bershadskii, A., & Niemela, J. J. (2004). Multiscale SOC in turbulent convection. *Physica A*, 340, 574-579.

Stanley, H. E., & Meakin, P. (1988). Multifractal phenomena in physics and chemistry. *Nature*, 335, 405-409.

Tebali, C. De Menech, M., & Stella, A. L. (1999). Multifractal scaling in the Bak-Tang-Wiesenfeld sandpile and edge events. *Physical review Letters*, 83, 3952-3955.

Thornton, T. L., & Gilden, D. L. (2005). Provenance of correlations in psychological data. *Psychonomic, Bulletin & Review*, 12(3), 409-441.

Torre, K., & Delignières, D. (2008). Unraveling the finding of $1/f^{\beta}$ noise in self-paced and synchronized tapping: a unifying mechanistic model. *Biological Cybernetics*, 99, 159-170.

Torre, K., Delignières, D., & Lemoine, L. (2007a). Detection of long-range dependence and estimation of fractal exponents through ARFIMA modelling. *British Journal of Mathematical and Statistical Psychology,* 60, 85-106.

Torre, K, Delignières, D., & Lemoine, L. (2007b). 1/*f*-fluctuations in bimanual coordination: An additional challenge for modeling. *Experimental Brain Research,* 183, 225-234.

Torre, K., & Wagenmakers, E. J., (2009). Theories and Models for $1/f^{\beta}$ noise in human movement science, *Human Movement Science*, 28, 297-318.

Uritsky, V. M., Paczuski M., Davila, J. M., & Jones, S. I. (2007). Coexistence of self-organized critically and intermittent turbulence in the solar corona. *Physical Review Letters*, 99, 025001.

Usher, M., Stemmler, M., & Olami, Z. (1995). Dynamic pattern formation leads to 1/*f* noise in neural populations. *Physical Review Letters*, 74, 326-329.

Van den Berg, J. C. (Ed.) (1999). *Wavelet in physics*. Cambridge: Cambridge University Press.

Van Orden, G. C., & Holden, J.G. (2002). Intentional contents and self-control. *Ecological Psychology,* 14, 87–109.

Van Orden, G. C., Holden, J. G., & Turvey, M. T. (2003). Self-organization of cognitive performance. *Journal of Experimental Psychology: General*, 132 (3), 331-350.

Van Orden, G. C., Holden, J. G., & Turvey, M. T. (2005). Human cognition and 1/ *f* scaling. *Journal of Experimental Psychology: General*, 134 (1), 117-123.

Veitch, D., & Abry, P. (1999). A wavelet-based joint estimator of the parameters of long-range dependence. *IEEE Transaction in Information Theory*, 45(3), 878-897.

Wagenmakers, E. J., Farrell, S., & Ratcliff, R. (2004). Estimation and interpretation of 1/*f*-noise in human cognition. *Psychonomic Bulletin and Review*, 11(4), 579-615.

Wagenmakers, E. J., Farrell, S., & Ratcliff, R. (2005). Human cognition and a pile of sand: A discussion on serial correlations and self-organized criticality. *Journal of Experimental Psychology: General,* 135, 108–116.

Walczak, B. (2000). *Wavelets in chemistry*, Amsterdam: Elsevier Science Publisher.

Ward, L. (2002). *Dynamical cognitive science*. Cambridge, MA: MIT press.

Whitcher, B. (1998). *Assessing nonstationary time series using wavelets*. Ph. D. dissertation, Department of Statistics, University of Washington, Seattle.

Wigner, E. (1932). On the quantum correction for thermodynamic equilibrium. *Physical Review*, 40, 749-759.

Wijnants, M. L., Bosman, A. M., Hasselman, F., Cox, R. F., & Van Orden, G. C. (2009). 1/f Scaling in movement time changes with practice in precision aiming. *Nonlinear Dynamics, Psychology, and the Life Sciences*, 13(1), 79-98.

Wing, A. L., & Kristofferson, A. B. (1973). The timing of interresponse intervals. *Perception and Psychophysics*, 13, 455-460.

Zapperi, S., Lauritsen, K. B., & Stanley, H. E. (1995). Self-organized branching processes. Mean-field theory of avalanches. *Physical Review Letters*, 75, 4071-4074.

Appendix

Symbols and abbreviations

t	Time (Euclidian time)
$\boldsymbol{x}$	Space (Euclidian space)
Δt	Temporal scale
Δx	Spatial scale
$1/f$	Inverse frequency, the same as scale Δt
$\Delta t \rightarrow 0$	When the time scale goes to zero
$A(t)$	Multifractal time
$A(\boldsymbol{x})$	Multifractal space
$dA(t)$	Increments in multifractal time
$B_H(t)$	Fractional Brownian motion or monofractal random walk
$B_H(A(t))$	Multifractal random walk
$\Delta B_H(t)$	Fractional Gaussian noise
$\Delta B_H(A(t))$	Multiplicative cascading process
$C_{\Delta t}(t)$	A cone in the time-scale plane
$D(h)$	The multifractal spectrum
$G(H \ln M)$	The probability density function of $H \ln M$
$H \ln M$	The logarithm of the interaction multipliers as a power law of the Hurst exponent (i.e., $H \ln M = \ln M^H$)
H	Hurst exponent
h	Singularity exponent
$h_{\max} - h_{\min}$	Multifractal spectrum width
$M_{\Delta t}(t)$	Interaction multipliers

$m_{\Delta t}(q)$	The q-order statistical moment of the wavelet coefficients $W_{\Delta t}(t)$
$P_{\Delta t}(\Delta X)$	The probability density function of $\Delta X_{\Delta t}(t)$ at temporal scale Δt
$W_{\Delta t}(t)$	Wavelet coefficient at scale Δt and time t
$\Delta X_{\Delta t}(t)$	Scale-dependent increments
$\zeta(q)$	Multiscaling exponent
AR	Autoregressive
CWT	Continuous Wavelet Transform
MODWT	Maximum Overlap Discrete Wavelet Transformation
RSI	Response to Stimulus Interval

Multiplicative interactions between temporal scales

In the present paper, the term 'interaction-dominant dynamics' are equated with 'multiplicative interactions between temporal scales' that generate intermittent fluctuations in a response series. This appendix provides the mathematical details that 'multiplicative interactions between temporal scales' imply the presence of 'multifractality' when the intermittent fluctuations are scale invariant. The mathematically less advanced reader can jump to the concluding remarks at the end of the section and read the implications of the introduced framework for the analysis of a response series. The mathematical theorems and proofs for this reasoning are found elsewhere (Bacry, & Muzy, 2003; Bacry, Muzy, & Delour, 2001; Bacry, Kozhemyak, & Muzy, 2008; Muzy & Bacry, 2002; Muzy, Bacry, & Kozhemyak, 2006).

Mathematical details: Statistically, the monofractal process of $1/f^{\alpha}$ fluctuation is defined as fractional Gaussian noise $\Delta B_H(t)$ (Mandelbrot & van Ness, 1968). $\Delta B_H(t)$ is equivalent with

the stationary increments of fractional Brownian motion $B_H(t)$ such that $\Delta B_H(t) = B_H(t+1) - B_H(t)$. The Hurst exponent H denotes the level of regularity and is related to the $1/f^{\alpha}$ power law by $\alpha = 2H - 1$. Thus, when $0 < H < 0.5$ or $-1 < \alpha < 0$ the fractional Gaussian noise $\Delta B_H(t)$ is anti-correlated (irregular), while it is long-range correlated (regular) when $0.5 < H < 1$ or $0 < \alpha < 1$. The scale-dependent increments $\Delta X_{\Delta t}(t) = B_H(t+\Delta t) - B_H(t)$ of fractional Brownian motion $B_H(t)$ were shown by Mandelbrot and van Ness (1968) to relate to each other by the following power law:

$$\Delta X_{\ell \Delta t}(\ell t) = \ell^H \Delta X_{\Delta t}(t) \tag{A1a}$$

where $\ell = \Delta t / T$ is the scaling factor, and T is the coarsest scale considered. Equation (A1a) implies that the probability density function of the scale-dependent increments $\Delta X = \Delta X_{\Delta t}(t)$ scales in a similar way:

$$P_{\Delta t}(\Delta X) = \ell^H P_{\ell \Delta t}(\ell^H \Delta X) \tag{A1b}$$

Consequently, since fractional Gaussian noise $\Delta B_H(t)$ has a Gaussian probability density function, so has its scale-dependent processes $\Delta X_{\Delta t}(t)$.

When multiplicative interactions between temporal scales generate intermittency in a response series, the fractional Gaussian noise has to be extended to a multiplicative cascading process (Muzy & Bacry, 2002). The *multiplicative cascading process* used in the present paper is the extension $\Delta B_H(A(t)) = B_H(A(t+1)) - B_H(A(t))$ of fractional Gaussian noise $\Delta B_H(t) = B_H(t+1) - B_H(t)$ when it evolves over multifractal time $A(t)$ (Mandelbrot, 1997). The multifractal time $A(t)$ is the cumulative product $dA(t)$ of interaction multipliers $M_{\Delta t}(t)$ within

the cone $C_{\Delta t}(t)$ integrated along the time axis when $\Delta t \to 0$ (Muzy & Bacry, 2002) (see Figure A1):

$$A(t) = \lim_{\Delta t \to 0} \int dA(t) \tag{A2a}$$

where:

$$dA(t) = \prod_{(\Delta t, t) \in C_{\Delta t}(t)} M_{\Delta t}(t) \tag{A2b}$$

The power law relation (A1a) between the temporal scales in the fractional Gaussian noise $\Delta B_H(t)$ is then generalized to the following equation for the multiplicative cascading process $\Delta B_H(A(t))$:

$$\Delta X_{\ell \Delta t}(\ell t) = \left[M_{\ell}(t) \right]^H \Delta X_{\Delta t}(t) \qquad \text{for} \qquad 0 < \Delta t \le T \tag{A3a}$$

which implies the following generalization of equation (A1b) (Castaing, Gagne, & Hopfinger, 1990):

$$P_{\Delta t}\left(\Delta X\right) = \int G_{\ell}(H \ln M)\, M^{-H} P_T\left(M^{-H} \Delta X\right) d(H \ln M) = G_{\ell}(H \ln M) \otimes P_T(\Delta X) \tag{A3b}$$

Equation (A3b) states that the probability density function $P_{\Delta t}(\Delta X)$ of the scale-dependent process $\Delta X_{\Delta t}(t)$ is a superposition of the probability density function $M^{-H} P_T(M^{-H} \Delta X)$ of the scale-dependent processes $\Delta X_T(t) = M^{-H} \Delta X$ at the coarsest scale T weighted by the

probability density function $G_{\ell}(H \ln M)$ of interaction multipliers. When no multiplicative interactions are present, $G_{\ell}(H \ln M)$ collapses into a single point such that interaction multipliers are equal to the temporal scale (i.e., $M = \Delta t$). In that case, the scaling relation (A1a-b) of fractional Gaussian noise is obtained as a special case of (A3a-b) when multifractal time coincides with Euclidian time; $A(t) = t$.

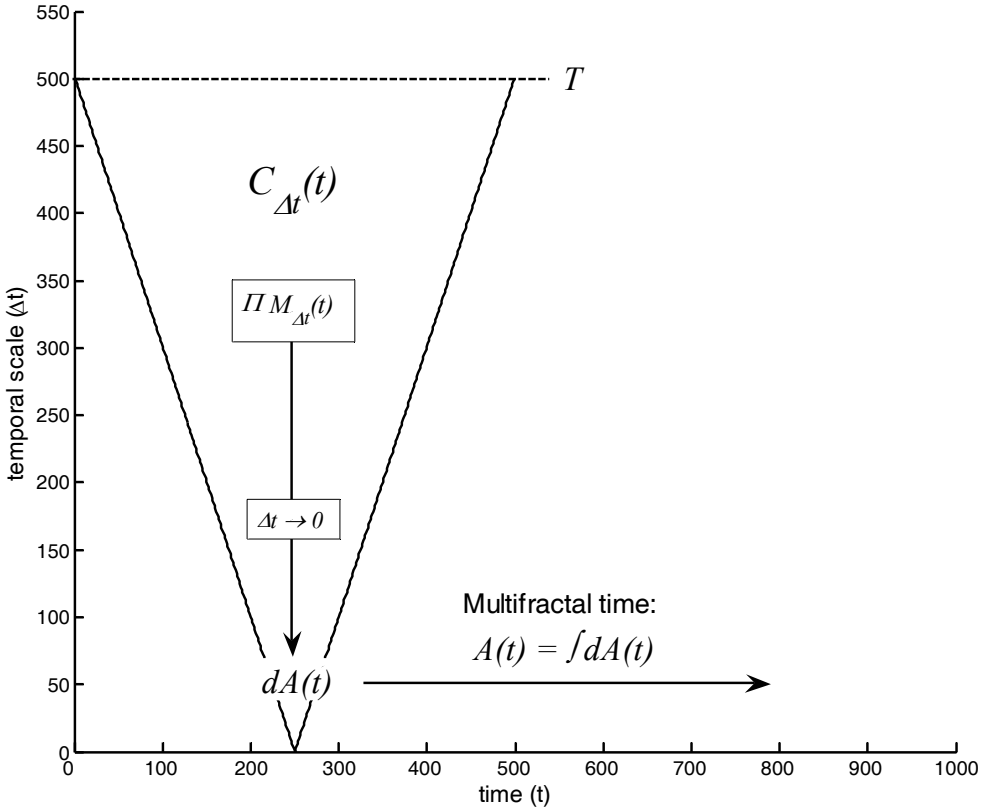

Figure A1. Illustration of the definition (A2a-b) of a multifractal time $A(t)$. $dA(t)$ is a cumulative product $\prod$ of the interaction multipliers $M_{\Delta t}(t)$ across cone $C_{\Delta t}(t)$ in the limit $\Delta t \to 0$, as symbolized by the downward arrow. Multifractal time $A(t)$ can then be defined as the integral $\int dA(t)$ over time t in the limit $\Delta t \to 0$ by translating the cone $C_{\Delta t}(t)$ across the time axis.

Equation (A3a-b) implies a non-Gaussian distribution of the multiplicative cascading process $\Delta B_H(A(t))$ such that the scaling of all q-order statistical moments has to be considered. The last equality of equation (A3b) states that the integral transformation can be rewritten as

the convolution product of the probability density function $G_{\ell}(H \ln M)$ of interaction multipliers and the probability density function $P_T(\Delta X)$ at the coarsest temporal scale T (Muzy & Bacry, 2002). The convolution product implies that q-order statistical moments $m_{\Delta t}(q)$ of probability density function $P_{\Delta t}(\Delta X)$ on a finer scale Δt are defined by the following equation:

$$\begin{aligned} m_{\Delta t}(q) &\overset{\text{Def}}{=} \int \Delta X^q P_{\Delta t}(\Delta X) d\Delta X \\ &= \int \Delta X^q G_{\ell}(H \ln M) \otimes P_T(\Delta X) d\Delta X \\ &\overset{\text{Def}}{=} \tilde{G}_{\ell}(q) \int \Delta X^q P_T(\Delta X) d\Delta X \\ &= \tilde{G}_{\ell}(q) m_T(q) \end{aligned} \qquad \text{(A4)}$$

The moment-generating function $\tilde{G}_{\ell}(q)$ is the Laplace transformation of $G_{\ell}(H \ln M)$ (third equality of equation (A4)) and relates the statistical moments $m_{\Delta t}(q)$ on scale Δt with the statistical moment $m_T(q)$ on the coarsest scale T. If the multiplicative interactions in Figure A1 are scale invariant, then $\tilde{G}_{\ell}(q) = \ell^{\zeta(q)}$ and the scaling of q-order statistical moments $m_{\Delta t}(q)$ below the coarsest temporal scale T yields the following power law (Bacry & Muzy, 2002):

$$m_{\Delta t}(q) = \ell^{\zeta(q)} m_T(q) \qquad \text{for} \qquad 0 < \Delta t \leq T \qquad \text{(A5)}$$

$\zeta(q)$ is a spectrum of multiscaling exponents which completely defines the distribution $G_{\ell}(H \ln M)$ of interaction multipliers when the multiplicative cascading process is scale invariant. The multifractal spectrum $D(h)$ is mathematically related to the spectrum of

multiscaling exponents $\zeta(q)$ through the Legendre transformation defined in equation (2) in the Methods section. $D(h)$ is the spectrum of dimensions $0 < D(h) < 1$ of the multifractal time $A(t)$ which collapses into the Euclidian time dimension $D(h) = 1$ when $A(t) = t$. In this special monofractal case, $\zeta(q) = qH$ is a linear function of q and the multiplicative cascading process $\Delta B_H(A(t))$ reduces to fractional Gaussian noise $\Delta B_H(t)$. In the present paper, the multiplicative cascading process was defined with a log-normal probability density function $G_{\ell}(H \ln M)$ of interaction multipliers, which yields (see Figure A2):

$$G_{\ell}(H \ln M) = \frac{1}{\sqrt{2\pi\sigma^2}} e^{-\frac{(H \ln M)^2}{2\sigma^2}} \tag{A6}$$

such that the spectrum of multiscaling exponents $\zeta(q)$ are given by:

$$\zeta(q) = qH + \frac{\sigma^2}{2} qH - \frac{\sigma^2}{2} (qH)^2 \tag{A7}$$

This particular multiplicative cascading process $\Delta B_H(A(t))$ was chosen since it is one of the most extensively investigated cascades in the literature (e.g., Arneodo, Manneville, & Muzy, 1998; Bacry, & Muzy, 2003; Bacry et al., 2001; Bacry et al., 2008; Muzy & Bacry, 2002; Muzy et al., 2006). The difference in intermittent fluctuations between a log-normal cascading process $\Delta B_H(A(t))$ with $\sigma = 0.7$ and $H = 1$ and fractional Gaussian noise $\Delta B_H(t)$ (i.e., pink noise) with $\sigma = 0$ and $H = 1$ is illustrated in Figure A3 together with Figure 3 in the Methods section.

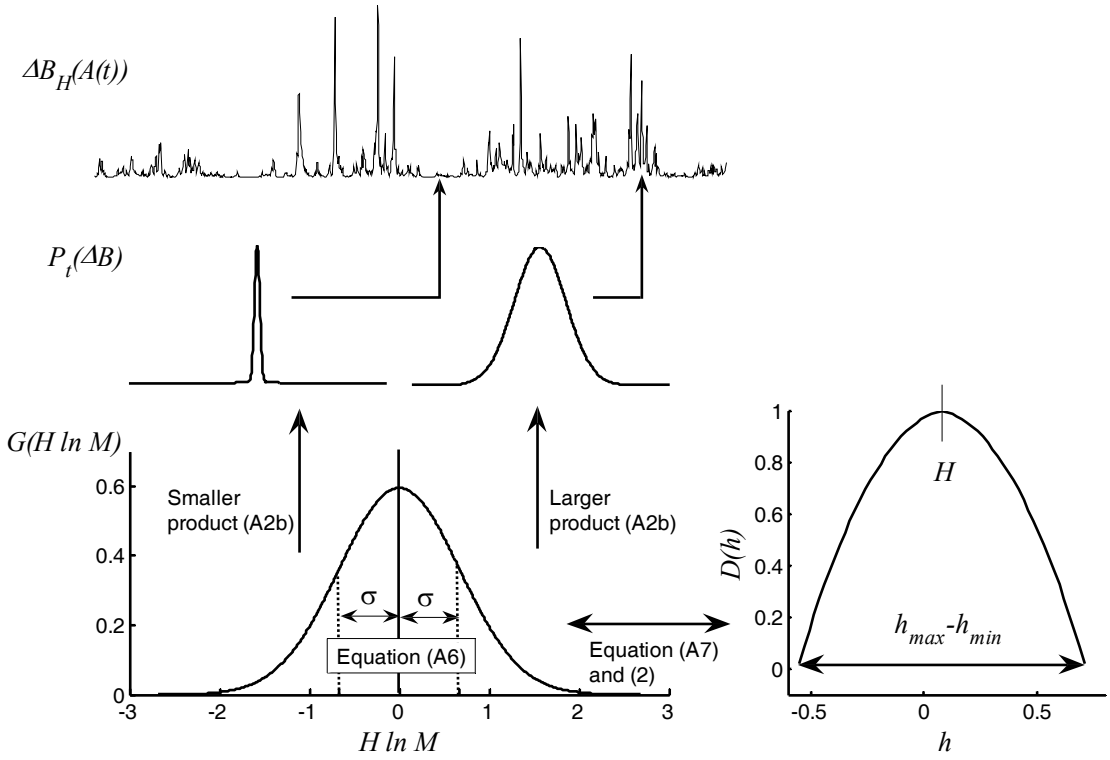

Figure A2: A summary of multiplicative cascading process $\Delta B(A(t))$. The *lower left panel* illustrates the distribution $G(H \ln M)$ of interaction multipliers assumed to be Gaussian (see equation (A6)). Through equations (A7) and (2), the width σ of $G(H \ln M)$ is related to the multifractal spectrum width $h_{\max} - h_{\min}$, as illustrated in the *lower right panel*. The width of local distribution $P_t(\Delta B)$ (*middle panel*) of $\Delta B(A(t))$ (*upper panel*) is dependent on whether the interaction multipliers of equation (A2b) are drawn from the left tail of $G(H \ln M)$ (i.e., small product of equation (A2b), *left arrow*) or the right tail (i.e., large product of equation (A2b), *right arrow*). Thus, the differences in the width of $P_t(\Delta B)$ of the laminar and intermittent periods of large and small variability is dependent on the width σ of $G(H \ln M)$ or, equivalently, the multifractal spectrum width $h_{\max} - h_{\min}$.

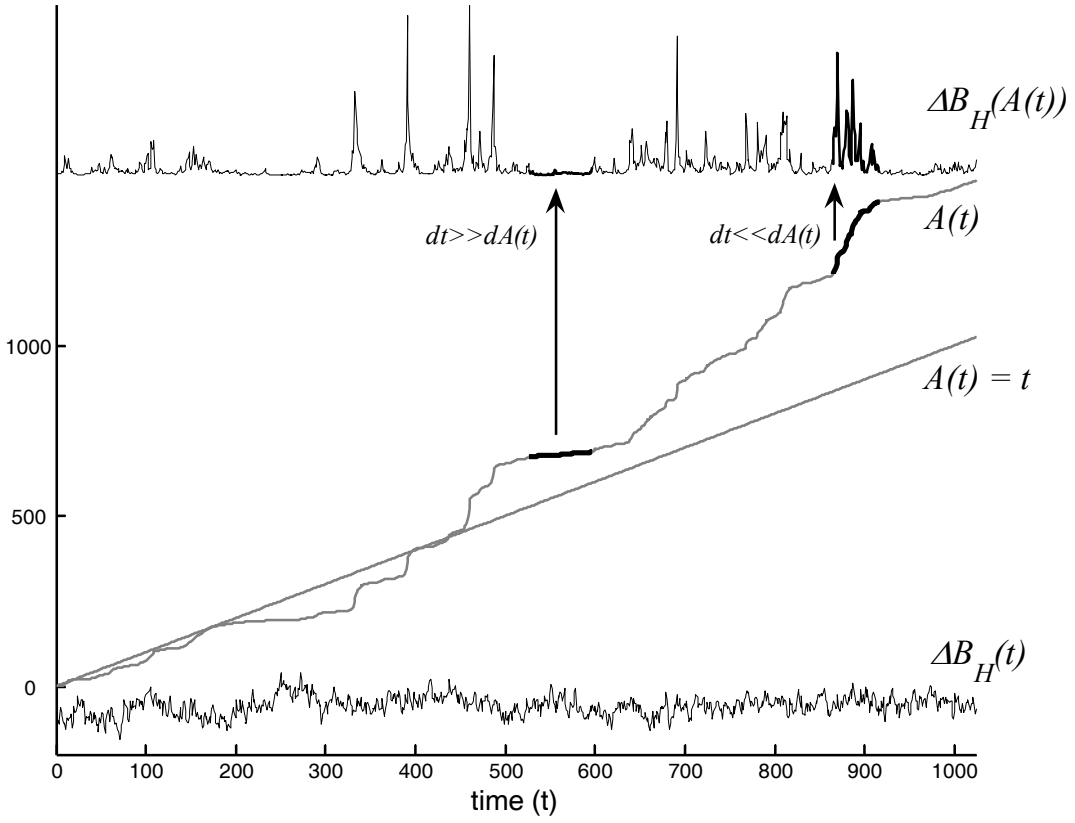

Figure A3. Illustration of the differences between multifractal time $A(t)$ and Euclidian time $A(t) = t$ for the multiplicative cascading process $\Delta B_H(A(t))$ with $H = 1$ (*upper trace*) and pink noise $\Delta B_H(t)$ also with $H = 1$ (*lower trace*). Periods of small and large variability emerge in a multiplicative cascading process $\Delta B_H(A(t))$ by deviation between multifractal time $A(t)$ and time t (*arrows*). These periods are not present in the special case of pink noise $\Delta B_H(t)$ where $A(t) = t$.

Concluding remarks: The mathematical reasoning above leads to several important remarks in the multifractal analysis and modeling of cognitive performance.

First, the identification of an α or H exponent of a response series cannot distinguish between an underlying multiplicative cascading process $\Delta B_H(A(t))$ and fractional Gaussian noise $\Delta B_H(t)$. This illustrates why methods like power spectrum analysis, detrended fluctuation analysis, rescaled range analysis, dispersion analysis and scale window variance analysis are blind to the interaction-generated structure of $A(t)$ and yield false positive results

in favor of a component-generated structure similar to $\Delta B_H(t)$. Consequently, the presence of intermittent or emerging response patterns caused by coordination between multiple time scales cannot be identified through a single α or H exponents. The intermittent periods of large performance variability generated by the multiplicative interactions between temporal scales of $\Delta B_H(A(t))$ are captured through the multifractal spectrum $D(h)$ instead.

Second, the multiplicative cascading process $\Delta B_H(A(t))$ is stationary (i.e., time independent) like fractional Gaussian noise $\Delta B_H(t)$. This is an extraordinary feature since both the local probability density function and regularity of $\Delta B_H(A(t))$ are time dependent (see Figure A3). The stationarity of $\Delta B_H(A(t))$ arises from the interrelation between its local amplitude and regularity. This means that large increments in $\Delta B_H(A(t))$ are counteracted by a large decrement that leads to intermittent periods of irregular fluctuations (i.e., a zigzag pattern) with large amplitude. In contrast, small increments evolve more freely and are not counteracted by concomitant decrements such that laminar periods with small and regular fluctuations emerge. Thus, the multiplicative cascading process $\Delta B_H(A(t))$ becomes a suitable model for the emergent changes in fluctuations in response series where its stationarity arises from the response time limits set by the task constraints.

Third, the H or α exponent defines the direction of the intermittent fluctuations generated by $A(t)$ in the multiplicative cascading process $\Delta B_H(A(t))$. In a cognitive task where the instruction "*respond as fast as possible*" is given, the intermittent periods of large performance variability will extend towards long response times since the laminar responses are fast. Consequently, long-range correlations (i.e., $H > 0.5$ or $\alpha > 0$) defines the right skew towards periods of intermittent slow responses. In the particular case $\alpha = H = 1$ for $\Delta B_H(A(t))$ used as example in Figures A2 and A3, almost all intermittent periods will go towards large response times which generates an asymmetric skew of the non-Gaussian probability density function (i.e., log-normal, power law probability density functions). In this particular case, the

structure of the multiplicative cascading process $\Delta B_H(A(t))$ is statistically equivalent to the structure of multifractal time $A(t)$ (e.g., $H = 1$ in equations (A6) and (A7)).

Fourth, the multiplicative cascading process $\Delta B_H(A(t))$ defined in the present paper assumes that the multiplicative interactions are scale invariant. According to the integral (A3b), this is not a necessary assumption, as it in general yields the following non-invariant scaling relation (e.g., Abry et al. 2002; Chainais et al., 2005):

$$m_{\Delta t}(q) = S(\ell)^{\zeta(q)} m_T(q) \qquad \text{for} \qquad 0 < \Delta t < T \tag{A8}$$

which reduces to equation (A5) when $\tilde{G}_\ell(q) = \ell^{\zeta(q)}$. Consequently, the present quantitative framework of interaction-dominant dynamics also includes fluctuations in response series that are not scale invariant, as previously reported in the literature (Wagenmakers et al., 2004).

Fifth, in the section Interaction-dominant dynamics in the human nervous system, the neural activation as a multiplicative cascading process $\Delta B_H(A(\boldsymbol{x}))$ is defined over multifractal neural space $A(\boldsymbol{x})$. In this case, the width Δt of the cone $C_{\Delta t}(t)$ in Figure A1 becomes the diameter Δx of the shrinking sphere in the three dimensional space shown in Figure 11. Thus, by substituting Δt with Δx and time t with the vector of spatial coordinates $\boldsymbol{x}$, the above mathematics can be applied. Thus, Figure 12 illustrates the difference in intermittent clustering of neural activity between a log-exponential cascade $\Delta B_H(A(\boldsymbol{x}))$ with $H = 1$ and a surrogate generated by an iterated amplitude adjusted three dimensional Fourier transformation that has equal $1/f^{\alpha}$ power law (i.e., $H = 1$) and non-Gaussian probability density but lacks the multiplicative interactions that are apparent in $\Delta B_H(A(\boldsymbol{x}))$.

Sixth, there are other processes besides the multiplicative cascading process $\Delta B_H(A(t))$ that generate intermittent dynamics. Processes like the Kesten process (Kesten, 1973), generalized autoregressive process with conditional heteroskedasticity (Bollerslev, 1986) and

generalized diffusion processes (Frank, 2004) have all been shown to create intermittent fluctuations. However, the corner stone in the multiplicative cascading process $\Delta B_H(A(t))$ is the ability to create intermittent fluctuations by multiplicative interactions between temporal scales which are not considered by the other models.

Wavelet-based multifractal analysis

To define the presence of multiplicative interactions in a response series, the spectrum of multiscale exponents $\zeta(q)$ or multifractal spectrum $D(h)$ has to be computed from the response series. The mathematical definition of a multiplicative cascading process $\Delta B_H(A(t))$ implies that the relationship between scale-dependent processes $\Delta X_{\Delta t}(t)$ equals the relationship between wavelet coefficients $W_{\Delta t}(t)$ such that $\Delta X_{\Delta t}(t) = W_{\Delta t}(t)$ in equation (A3b). In the present section, two algorithms for the definition of wavelet coefficients are defined, Continuous Wavelet Transformation (CWT) and Maximum Overlap Discrete Wavelet Transformation (MODWT), before the multiscaling exponents $\zeta(q)$ and multifractal spectrum $D(h)$ are computed from the obtained wavelet coefficients. Finally, the *D*-statistics identify the presence of inhomogeneous wavelet variance that arises from a multiplicative cascading process $\Delta B_H(A(t))$. The reader is advised to consider the concluding remarks before applying the presently introduced framework to response series.

Continuous Wavelet Transform (CWT): Let $X(t)$ be a response series with $t = 1, 2, \ldots, N$ trials. Let $\psi(t/\Delta t)$ be the Morlet waveform scaled according to scale Δt illustrated in the upper panel of Figure 2A. Then the wavelet coefficients $W_{\Delta t}(t)$ of CWT are defined according to the following equation:

$$W_{\Delta t}(t) = \frac{1}{\sqrt{\Delta t}} \int X(t)\psi(t/\Delta t)dt \qquad \text{(A9)}$$

High $W_{\Delta t}(t)$ denotes high correlation between the Morlet waveform $\psi(t/\Delta t)$ and the response series $X(t)$ within the cone $C_{\Delta t}(t)$ of the upper panel of Figure 2A. Thus, normalizing the signal energy to 1, the wavelet coefficient $W_{\Delta t}(t)$ defines the time-dependent correlation coefficients between the Morlet waveform and the response series $X(t)$ for each temporal scale Δt.

Maximum Overlap Discrete Wavelet Transformation (MODWT): For MODWT the wavelet coefficients $W_{\Delta t}(t)$ are defined by the following algorithm (Percival & Walden, 2000):

$$W_{\Delta t}(t) = \sum_{l=0}^{L_{\Delta t}-1} h_{\Delta t,l} X(t - l \bmod N) \qquad \text{for} \qquad \Delta t = 2, 4.., 1024 \quad \text{and } t = 0,\ldots,1023 \qquad \text{(A10)}$$

where the waveform illustrated in the lower panel of Figure 2A is defined by the filter coefficients G_l for $l = [0, 1,\ldots, 7]$ for an 8th order Least Asymmetric filter (see Table 109 in Percival and Walden, 2000):

$$h_{\Delta t,l} = \frac{G_{L-l}(-1)^l}{2^{\log_2(\Delta t)/2}} \qquad \text{(A11)}$$

The upper limit $L_{\Delta t} = 6\Delta t + 5$ in the sum of equation (A10) defines the length of the waveform in the lower panel of Figure 2A and the argument $t - l \bmod N$ the centering of the waveform in the middle of the cone $C_{\Delta t}(t)$ with width Δt. The 8th order Least Asymmetric waveform was chosen since it prevents energy leakage into adjacent scales Δt without inducing a high filter

order. High filter orders extend the region between the ends of the cone $C_{\Delta t}(t)$ and the ends of the waveform, which induces artifacts into a large number of samples at the endpoints of the response series. The wavelet transformation in the present paper was confined to scales Δt = 2, 4, 8, 16 and 32 trials in order to prevent the influence of these boundary coefficients. In contrast to the CWT, the MODWT is able to define scale-dependent processes illustrated in the lower panel of Figure 2B as orthogonal components represented by the inverse MODWT:

$$D_{\Delta t}(t) = \sum_{l=0}^{L_{\Delta t}-1} h_{\Delta t,l} W_{\Delta t}(t - l \bmod N) \quad \text{for} \quad \Delta t = 2,4,...,1024 \quad \text{and} \quad t = 0,...,1023 \tag{A12}$$

Computation of the multifractal spectrum: The multifractal spectrum of the response time series is obtained by the Legendre transform (2) after the multiscaling exponents $\zeta(q)$ has been computed as the linear slope of the least square fit of $\log_2 m_{\Delta t}(q)$ versus $\log_2 \Delta t$. However, a weighted least square fit is employed for the MODWT based estimation since its limited number of discrete scales Δt limits the precision of the ordinary least square fit. The weighted least square fit is computed by the following two steps. First, the q-order statistical moment $m_{\Delta t}(q)$ in equation (A5) is computed by the wavelet coefficients $W_{\Delta t}(t)$ obtained from equation (A10):

$$\begin{aligned} k_{\Delta t}(q,t) &= \left|W_{\Delta t}(t)\right|^q \\ m_{\Delta t}(q) &= \frac{1}{N - 2n_{\Delta t}} \sum_{t=1}^{N} k_{\Delta t}(q,t) \end{aligned} \tag{A13}$$

where $n_{\Delta t} = (5\Delta t+5)/2$ initial and end points were inflicted by boundary artifacts and excluded. Secondly, the multiscale exponents $\zeta(q)$ for $0 < q < 3$ is estimated by a weighted least squares estimation (Veitch & Abry, 1999; Abry et al., 2000, 2002):

$$\zeta(q) = \sum_{\Delta t} \frac{\left(w_1(q)\Delta t - w_2(q)\right) Y_{\Delta t}(q)}{\left(w_1(q)w_3(q) - \left(w_2(q)\right)^2\right) X_{\Delta t}(q)} \tag{A14}$$

with weights:

$$\begin{aligned} w_1(q) &= \sum_{\Delta t} \frac{1}{X_{\Delta t}(q)} \\ w_2(q) &= \sum_{\Delta t} \frac{\log_2 \Delta t}{X_{\Delta t}(q)} \\ w_3(q) &= \sum_{\Delta t} \frac{(\log_2 \Delta t)^2}{X_{\Delta t}(q)} \end{aligned} \tag{A15}$$

$X_{\Delta t}(q)$ and $Y_{\Delta t}(q)$ were estimated under the general assumption that the response series has a non-Gaussian distribution with finite variance:

$$X_{\Delta t}(q) = \frac{\left(\log_2 e\right)^2 V_{\Delta t}(q)}{N - 2n_{\Delta t}} \tag{A16}$$

$$Y_{\Delta t}(q) = \log_2 m_{\Delta t}(q) + \frac{\log_2 e \; V_{\Delta t}(q)}{N - 2n_{\Delta t}} - \frac{q \log_2 \Delta t}{2}$$

with:

$$V_{\Delta t}(q) = \frac{\left[std_t \left(\log_2 k_{\Delta t}(q,t) \right) \right]^2}{\left[mean_t \left(\log_2 k_{\Delta t}(q,t) \right) \right]^2} \tag{A17}$$

where $m_{\Delta t}(q)$ and $k_{\Delta t}(q,t)$ is defined by equation (A13).

D-statistics of wavelet variance: The following equations (A18) - (A22) provide a general test statistics for the stationarity of the wavelet variance $\left[W_{\Delta t}(t)\right]^2$ of each temporal scale Δt (Whitcher, 1998):

$$D = \max\left(D_{-}, D_{+}\right) \tag{A18}$$

where:

$$D_{\pm} = \max_k\left(\Delta_k^{\pm}\right) \tag{A19}$$

where:

$$\Delta_k^{+} = \frac{k - n_{\Delta t} + 2}{N - n_{\Delta t}} - P_k \qquad \Delta_k^{-} = P_k - \frac{k - n_{\Delta t} + 1}{N - n_{\Delta t}} \tag{A20}$$

where:

$$P_k = \frac{\sum_{t=n_{\Delta t}-1}^{k}\left[W_{\Delta t}(t)\right]^2}{\sum_{t=n_{\Delta t}-1}^{N-1}\left[W_{\Delta t}(t)\right]^2} \qquad \text{for} \qquad k = n_{\Delta t} - 1, \ldots, N-2 \tag{A21}$$

where $n_{\Delta t} = (5\Delta t+5)/2$ initial points were inflicted by boundary artifacts and excluded. In order to decide whether D is significantly different from a homogenous wavelet variance, D_{surr} is computed for N series of Gaussian-distributed random numbers. N' then defines the number

of series for which $D_{surr}>D$, and the response series has a significant inhomogeneous wavelet variance if:

$$\frac{N'}{N} < 0.05 \tag{A22}$$

By substituting the Gaussian random numbers with N realizations of a superposition of $1/f^{\alpha}$ fluctuation and white noise, an aggregated autoregressive model, or a multiplicative cascading process, one creates a statistical test for the significant resemblance between the probability density function of $W_{\Delta t}(t)$ on each scale Δt in a response series and each of these models.

Concluding remarks: The following remarks are important to consider when wavelet-based multifractal analysis is applied to response series.

First, there are other transformations besides wavelets that decompose a response series into the time-scale plane of Figure 2. There are, for example, the short-time Fourier transformation (Gabor, 1946), the Hilbert transform combined with either Fourier band-pass decomposition (Bloomfield, 1976), empirical mode decomposition (Huang, Shen, Long, Wu, Shih, Zheng, Yen, Tung, & Liu, 1998), or wavelet packet decomposition (Ihlen, 2009; Olhede & Walden, 2005), and the Wigner-Ville transform (Wigner, 1932), to name but a few. The wavelet approach was chosen in the present paper because it is the most utilized transformation in the multifractal analysis of multiplicative cascading processes.

Secondly, although the deduction of the multifractal spectrum width $h_{\max} - h_{\min}$ was validated by two different wavelet algorithms, the estimated spectrum was restricted to a limited range $0 < q < 3$ of q-order statistical moments (A13). The upper bound was set through tests on sets of 100 realizations of log-normal cascades (A6) of 1024 samples, where each set was within a large range of spectrum widths (see the gray arcs in Figure 3C). The

estimation error increases for higher order q in the statistical moments by the finite size of the synthesized series. However, the slope q of the multifractal spectrum $D(h)$ yields less increase in h and therefore less influence on the spectrum width $h_{max} - h_{min}$ for higher order q. Furthermore, Lashermes, Abry, and Chainais (2004) have shown that there is a linearization effect for the wavelet-based estimation of the multiscaling exponent $\zeta(q)$ for large q that further advocates the restrictive range used in the present study. The lower bound $q > 0$ was chosen since both the CWT and MODWT utilized in the present study yield unstable estimations of negative moments of equation (A13) (e.g., Manimaran, Panigrahi, & Parikh, 2005). This implies that only the lower half of the spectrum is estimated (see Figures 5C, 6D and 7B), which assumes a symmetric distribution $G(H \ln M)$ of the interaction multipliers. Modulus maxima extensions of the CWT (Muzy et al., 1993) and multifractal extensions of detrended fluctuation analysis (Kantelhardt, Zschiegner, Koscielny-Bunde, Havlin, Bunde, & Stanley, 2002) have been shown to yield stable estimations of the multifractal spectrum for negative q. Unfortunately, even a series of 1024 trials as in the current data sets is not enough to yield stable results for these analyses, which would need in the order of 3000 - 8000 trials. However, the negative q defines the scaling of the laminar periods with low performance variability, the precision of which is limited by the millisecond accuracy of the response time measurements. Possible alternatives to extend the estimation of the multifractal spectrum width such that it can include the negative q-range are a MODWT using wavelet leaders rather than coefficients (cf. Jaffard, Lashermes, & Abry, 2006) or an indirect estimation by applying conventional monofractal methods to the magnitude of change in response time (cf. Ashkenazy, Havlin, Ivanov, Peng, Frohlinde, & Stanley, 2003; Kalisky, Ashkenazy, & Havlin, 2005).

Thirdly, both the MODWT and CWT algorithms assume that the multiplicative interactions are scale invariant such that the weighted linear least square fit (A13)-(A17) can

estimate the multiscaling exponent $\zeta(q)$. Only when this assumption holds can multifractality be unequivocally equated with intermittency generated by multiplicative interactions between temporal scales. However, this assumption does not necessarily hold for all response series across cognitive tasks. There were several signs of deviations from strict multifractal fluctuations in the present reanalyses. First, several of the response series had a multifractal spectrum width $h_{\min} - h_{\max}$ significantly smaller then the surrogate series while the presence of multifractality predicts that the width should be significantly larger. Secondly, the lower panel in Figure 5C displays a response series of an interval estimation task that possesses an approximately monofractal spectrum. Yet, the wavelet coefficients $W_{\Delta t}(t)$ of the MODWT (A10) of the same response series are more inhomogeneously distributed (see lower panel of Figure 5A) compared to the fractional Gaussian noise $\Delta B_H(t)$ in lower panels in Figure 3. Thirdly, all 66 response series had wavelet variances significantly ($p < 0.05$) different from a Gaussian noise by the *D*-statistics (A18)-(A22), although some of the series especially in the interval estimation and word naming task had a monofractal spectrum in addition. These three signs contradict the omnipresence of multifractal fluctuations in cognitive performance. However, it does not necessarily contradict the omnipresence of multiplicative interactions between temporal scales. The significantly larger ensemble of multifractal spectrum widths for the surrogates still indicates that interrelation between the Fourier phases of certain response series influences the multifractal spectrum width. However, these interrelations might be more local in scale as seen in the lower panel of Figure 5A compared with the interrelations seen in a multiplicative cascading process $\Delta B_H(A(t))$ (see upper panel of Figure 3A). Actually, the response series in the lower panels of Figure 5A was one of the few response series where the inhomogeneous variance was not well replicated by a multiplicative cascading process $\Delta B_H(A(t))$ with equal multifractal spectrum width $h_{\min} - h_{\max}$. Thus, it is important to note that multifractal analyses compress the information of the multiplicative

interactions (i.e., interrelation between the Fourier phases) in the time-scale plane into the multifractal spectrum width under the assumption that the response time fluctuations are scale invariant. Further development of time-scale decomposition, multifractal analysis and multiplicative cascading models is important for application to response series where the multiplicative interactions between temporal scales are not scale invariant.